

1 **Nitrogen Fixation in Arctic Coastal Waters (Qeqertarsuaq, West**
2 **Greenland): Influence of Glacial Melt on Diazotrophs, Nutrient**
3 **Availability, and Seasonal Blooms**

4 Schlangen Isabell¹, Leon-Palmero Elizabeth^{1,2}, Moser Annabell¹, Xu Peihang¹, Laursen Erik¹, and
5 Löscher Carolin R.^{1,3}

6 ¹Nordceee, Department of Biology, University of Southern Denmark, Campusvej 55, 5230 Odense M, Denmark

7 ²Department of Geosciences, Princeton University, Princeton, New Jersey

8 ³DIAS, University of Southern Denmark, Odense, Denmark

9 **Correspondence:** Carolin R. Löscher (cloescher@biology.sdu.dk)

10
11 **Abstract.** The Arctic Ocean is undergoing rapid transformation due to climate change, with decreasing sea ice contributing to
12 a predicted increase in primary productivity. A critical factor determining future productivity in this region is the availability
13 of nitrogen, a key nutrient that often limits biological growth in Arctic waters. The fixation of dinitrogen (N₂) gas, a biological
14 process mediated by diazotrophs, not only supplies new nitrogen to the ecosystem but also plays a central role in shaping
15 the biological productivity of the Arctic. Historically it was believed to be limited to oligotrophic tropical and subtropical
16 oceans, Arctic N₂ fixation has only garnered significant attention over the past decade, leaving a gap in our understanding
17 of its magnitude, the diazotrophic community, and potential environmental drivers. In this study, we investigated N₂ fixation
18 rates and the diazotrophic community in Arctic coastal waters, using a combination of isotope labeling, genetic analyses and
19 biogeochemical profiling, in order to explore its response to glacial meltwater, nutrient availability and its impact on primary
20 productivity. Here we show N₂ fixation rates ranging from 0.16 to 2.71 nmol N L⁻¹ d⁻¹, to be notably higher than those observed
21 in many other oceanic regions, suggesting a previously unrecognized significance of N₂ fixation in these high-latitude waters.
22 The diazotrophic community is predominantly composed of UCYN-A. We found highest N₂ fixation rates co-occurring with
23 maximum chlorophyll *a* concentrations and primary production rates at a station in the Vaigat Strait close impacted by glacier
24 meltwater inflow, possibly providing otherwise limiting nutrients. Our findings illustrate the importance of N₂ fixation in an
25 environment previously not considered important for this process and provide insights into its response to the projected melting
26 of the polar ice cover.

27
28 **1 Introduction**

29
30 Nitrogen is a key element for life and often acts as a growth-limiting factor for primary productivity (Gruber and Sarmiento,
31 1997; Gruber, 2004; Gruber and Galloway, 2008). Despite nitrogen gas (N₂) making up approximately 78% of the atmosphere,
32 it remains inaccessible to most marine life forms. Diazotrophs, which are specialized bacteria and archaea, have the ability to
33 convert N₂ into biologically available nitrogen, facilitated by the nitrogenase enzyme complex carrying out the process of
34 biological nitrogen fixation (N₂ fixation) (Capone and Carpenter (1982)). Despite the fact that these organisms are highly spe-

35 cialized and N₂ fixation is energetically demanding, the ability to carry out this process is widespread amongst prokaryotes.
36 However, it is controlled by several factors such as temperature, light, nutrients and trace metals such as iron and molybdenum
37 (Sohm et al., 2011; Tang et al., 2019). Oceanic N₂ fixation is the major source of nitrogen to the marine system (Karl et al.,
38 2002; Gruber and Sarmiento, 1997), thus, diazotrophs determine the biological productivity of our planet (Falkowski et al.
39 (2008), impact the global carbon cycle and the formation of organic matter (Galloway et al., 2004; Zehr and Capone, 2020).
40 Traditionally it has been believed that the distribution of diazotrophs was limited to warm and oligotrophic waters (Buchanan
41 et al., 2019; Sohm et al., 2011; Luo et al., 2012) until putative diazotrophs were identified in the central Arctic Ocean and
42 Baffin Bay (Farnelid et al., 2011; Damm et al., 2010). First rate measurements have been reported for the Canadian Arctic by
43 Blais et al. (2012) and recent studies have reported rate measurements in adjacent seas (Harding et al., 2018; Sipler et al., 2017;
44 Shiozaki et al., 2017, 2018), drawing attention to cold and temperate waters as significant contributors to the global nitrogen
45 budget through diverse organisms.

46 N₂ fixation is performed by diverse group of cyanobacteria as well as by non-cyanobacteria diazotrophs (NCDs). UCYN-A
47 has been described as the dominant active N₂ fixing cyanobacterial diazotroph in arctic waters (Harding et al. (2018)), while
48 other cyanobacteria have only occasionally been reported (Díez et al., 2012; Fernández-Méndez et al., 2016; Blais et al., 2012).
49 Recent studies found that the majority of the arctic marine diazotrophs are NCDs and those may contribute significantly to N₂
50 fixation in the Arctic Ocean (Shiozaki et al., 2018; Fernández-Méndez et al., 2016; Harding et al., 2018; Von Friesen and Rie-
51 mann, 2020). Still, studies on the Arctic diazotroph community remain scarce, leaving Arctic environments poorly understood
52 regarding N₂ fixation. Shao et al. (2023) note the impossibility of estimating Arctic N₂ fixation rates due to the sparse spatial
53 coverage, which currently represents only approximately 1 % of the Arctic Ocean. Increasing data coverage in future studies
54 will aid in better constraining the contribution of N₂ fixation to the global oceanic nitrogen budget (Tang et al. (2019)).

55 The Arctic ecosystem is undergoing significant changes driven by rising temperatures and the accelerated melting of sea ice, a
56 trend, predicted to intensify in the future (Arrigo et al., 2008; Hanna et al., 2008; Haine et al., 2015). These climate-driven shifts
57 have stimulated primary productivity in the Arctic by 57 % from 1998 to 2018, elevating nutrient demands in the Arctic Ocean
58 (Ardyna and Arrigo, 2020; Arrigo and van Dijken, 2015; Lewis et al., 2020). This increase is attributed to prolonged
59 phytoplankton growing seasons and expanding ice-free areas suitable for phytoplankton growth (Arrigo et al. (2008)).

60 However, despite these dramatic changes, the role of N₂ fixation in sustaining Arctic primary production remains poorly
61 understood. While recent studies suggest that diazotrophic activity may contribute to nitrogen inputs in polar regions (Sipler
62 et al. (2017)), fundamental uncertainties remain regarding the extend, distribution and environmental drivers of N₂ Fixation in
63 the Arctic Ocean. Specifically, it is unclear whether increased glacial meltwater input enhances or inhibits N₂ Fixation through
64 changes in nutrient availability, stratification, and microbial community composition. Thus, the question of whether nitrogen
65 limitation will emerge as a key factor constraining Arctic primary production under future climate scenarios remains unresolved. In this
66 study, we investigate the diversity of diazotrophic communities alongside in situ N₂ fixation rate measurements in Disko Bay
67 (Qeqertarsuaq), a coastal Arctic system strongly influenced by glacial meltwater input. By linking environmental parameters to N₂
68 fixation dynamics, we aim to clarify the role of diazotrophs in Arctic nutrient cycling and assess their potential contribution to

Deleted: in those waters

Deleted: Additionally, t

Deleted: consequent reduc- tion

Deleted: in

Formatted: Indent: Left: 0,14 cm, Right: 0,66 cm

Deleted: extent due to accelerated melting, which is

Deleted: increase

Deleted: severe

Deleted: thereby

Deleted: can be

Deleted: the extension of the

Deleted: the

Deleted: sion of

Deleted:

Deleted: available

Deleted: The Greenland Ice Sheet is strongly affected by climate change and the waters of Baffin Bay have experienced a substantial sea surface temperature (SST) increase of 47.4 % along with a significant increase in chlorophyll *a* (Chl *a*) concentration of 26.4 % over the last two decades (1998–2018) (Lewis et al. (2020)). Coastal sites are particularly impacted by melting, receiving glacial runoff enriched with nutrients and trace elements triggering phytoplankton blooms and altering near-shore biogeochemical cycling (Ardyna and Arrigo, 2020; Arrigo et al., 2017; Hendry et al., 2019; Bhatia et al., 2013).

94 [sustaining primary production in a changing Arctic. Understanding these processes is essential for refining biogeochemical](#)
95 [models and predicting ecosystem responses to future climate change.](#)

96 **2 Material and methods**

97 **2.1 Seawater sampling**

100 The research expedition was conducted from August 16 to 26 in 2022 aboard the Danish military vessel P540 within the waters
101 of Qeqertarsuaq, located in the western region of Greenland (Kalaallit Nunaat). [Discrete water samples were obtained using a](#)
102 [10 L Niskin bottle, manually lowered with a hand winch to five distinct depths \(surface, 5, 25, 50, and 100 m\).](#) A comprehensive
103 sampling strategy was employed at 10 stations (Fig. 1), covering the surface to a depth of 100 m. The sampled parameters
104 included water characteristics, such as nutrient concentrations, chl *a*, particulate organic carbon (POC) and nitrogen (PON),
105 molecular samples for nucleic acid extractions (DNA), dissolved inorganic carbon (DIC) as well as CTD sensor data. At three
106 selected stations (3,7,10) N₂ fixation and primary production rates were quantified through concurrent incubation experiments.
107 Samples for nutrient analysis, nitrate (NO₃⁻), nitrite (NO₂⁻) and phosphate (PO₄³⁻) were taken in triplicates, filtered through
108 a 0.22 μ m syringe filter (Avantor VWR® Radnor, Pa, USA) and stored at -20 °C until further analysis. Concentrations were
109 spectrophotometrically determined (Thermo Scientific, Genesys 10S UV-VIS spectrophotometer) following the established
110 protocols of Murphy and Riley (1962) for PO₄³⁻; García-Robledo et al. (2014) for NO₃⁻ & NO₂⁻ ([detection limits: 0.01 \$\mu\$ mol](#)
111 [L⁻¹ \(NO₃⁻, NO₂⁻, and PO₄³⁻\), 0.05 \$\mu\$ mol L⁻¹ \(NH₄⁺\).](#) Chl *a* samples were filtered onto 47 mm ϕ GF/F filters (GE Healthcare
112 Life Sciences, Whatman, USA), placed into darkened 15 mL LightSafe centrifuge tubes (Merck, Rahway, NJ, USA) and were
113 subsequently stored at -20 °C until further analysis. To determine the Chl *a* concentration, the samples were immersed in 8
114 mL of 90 % acetone overnight at 5 °C. Subsequently, 1 mL of the resulting solution was transferred to a 1.5 mL glass vial
115 (Mikrolab Aarhus A/S, Aarhus, Denmark) the following day and subjected to analysis using the Trilogy® Fluorometer
116 (Model #7200-00) equipped with a Chl *a* in vivo blue module (Model #7200-043, both Turner Designs, San Jose, CA, USA).
117 Measurements of serial dilutions from a 4 mg L⁻¹ stock standard and 90 % acetone (serving as blank) were performed to
118 calibrate the instrument. In addition, measurements of a solid-state secondary standard were performed every 10 samples.
119 Water (1 L) water from each depth was filtered for the determination of POC and PON concentrations, as well as natural
120 isotope abundance (δ ¹³C POC / δ ¹⁵N PON) using 47 mm ϕ , 0.7 μ m nominal pore size precombusted GF/F filter (GE
121 Healthcare Life Sciences, Whatman, USA), which were subsequently stored at -20 °C until further analysis. Seawater samples
122 for DNA were filtered through 47 mm ϕ , 0.22 μ m MCE membrane filter (Merck, Millipore Ltd., Ireland) for a maximum of 20
123 minutes, employing a gentle vacuum (200 mbar). The filtered volumes varied depending
124 on the amount of material captured on the filter, ranging from 1.3 L to 2 L, with precise measurements recorded. The filters
125 were promptly stored at -20 °C on the ship and moved to -80 °C upon arrival to the lab until further analysis.

126 To achieve detailed vertical profiles, a conductivity-temperature-depth-profiler (CTD, Seabird X) equipped with supplement-
127 ary sensors for dissolved oxygen (DO), photosynthetic active radiation (PAR), and fluorescence (Fluorometer) was manually

Deleted: Given the changes, there is an urgency to explore the role of N₂ fixation in shaping the response of the Arctic ecosystem to these environmental changes. While the general magnitude of N₂ fixation is suspected to have a substantial impact (Sipler et al. (2017)), the complexity of Arctic biogeochemical processes necessitates further studies and broader spatial and temporal investigations to facilitate robust predictions. The question of whether primary

Deleted: production in the Arctic will be limited by nitrogen availability and the extent to which species will adapt to these conditions remains unknown and needs to be addressed. This study aims to contribute to the understanding of N₂ fixation dynamics and its implications for ecosystem productivity with the rapidly evolving Arctic Ocean.

We explored the diazotroph diversity in combination with N₂ fixation rate measurements, to elucidate the importance of this process in the Arctic ecosystem. We hope that understanding the dynamics of N₂ fixation and its impact on the ecosystem productivity can inform predictions and help managing the consequences of ongoing environmental changes in the Arctic Ocean. Our study has been carried out in Disko Bay (Qeqertarsuaq), which can serve as a model for Arctic coastal systems influenced by large meltwater runoff and thus potentially an addition of high levels of iron and nutrients, both of which have the ability to affect N₂ fixation (Lewis et al., 2020; Bhatia et al., 2013).

Deleted: -

Formatted: Superscript

Formatted: Subscript

Formatted: Superscript

Formatted: Subscript

Formatted: Superscript

Formatted: Subscript

Formatted: Superscript

Formatted: Subscript

Formatted: Superscript

Deleted: -

Deleted:

Deleted: Seawater (40 ml) was filtered through a 0.22 μ m syringe filter (Avantor VWR® Radnor, Pa, USA) and stored at 4 °C in an amber glass vial, sealed with closed caps, affixed with a PTFE-faced silicon liner (Thermo Fisher Scientific, Waltham, MA, USA) for subsequent DIC measurements in the laboratory using an AS-C5 DIC analyzer (ApolloSciTech, Newark, Delaware, USA) equipped with a laser-based CO₂ detector. Sample anal

179 deployed.

180 2.2 Nitrogen fixation and primary production

181 Water samples were collected at three distinct depths (0, 25 and 50 m) for the investigation of N₂ fixation rates and primary
182 production rates, encompassing the euphotic zone, chlorophyll maximum, and a light-absent zone. Three incubation stations
183 (Fig. 2: station 3, 7, 10) were chosen, in a way to cover the variability of the study area. This strategic sampling aimed to
184 capture a gradient of the water column with varying environmental conditions, relevant to the aim of the study. N₂ fixation
185 rates were assessed through triplicate incubations employing the modified ¹⁵N-N₂ dissolution technique after Großkopf et al.
186 (2012) and Mohr et al. (2010).

187 To ensure minimal contamination, 2.3 L glass bottles (Schott-Duran, Wertheim, Germany) underwent pre-cleaning and acid
188 washing before being filled with seawater samples. Oxygen contamination during sample collection was mitigated by gently
189 and bubble-free filling the bottles from the bottom, allowing the water to overflow. Each incubation bottle received a 100 mL
190 amendment of ¹⁵N-N₂ enriched seawater (98 %, Cambridge Isotope Laboratories, Inc., USA) achieving an average dissolved
191 N₂ isotope abundance (¹⁵N atom %) of 3.90 ± 0.02 atom % (mean \pm SD). Additionally, 1 mL of H^3CO_3 (1g/50 mL) (Sigma-
192 Aldrich, Saint Louis Missouri US) was added to each incubation bottle, roughly corresponding to 10 atom % enrichment and
193 thus measurements of primary production and N₂ fixation were conducted in the same bottle. Following the addition of both
194 isotopic components, the bottles were closed airtight with septa-fitted caps and incubated for 24 hours on-deck incubators with
195 a continuous surface seawater flow. These incubators, partially shaded ([using daylight-filtering foil](#)) to simulate in situ
196 photosynthetically active radiation (PAR) conditions, aimed to replicate environmental parameters experienced at the sampled
197 depths. Control incubations utilizing atmospheric air served as controls to monitor any natural changes in δ ¹⁵N not attributable
198 to ¹⁵N-N₂ addition. These control incubations were conducted using the dissolution method, like the ¹⁵N-N₂ enrichment
199 experiments, but with the substitution of atmospheric air instead of isotopic tracer.

200 After the incubation period, subsamples for nutrient analysis were taken from each incubation sample, and the remaining
201 content was subjected to the filtration process and were gently filtered (200 mbar) onto precombusted GF/F filters (Advantec,
202 47 mm ø, 0.7 μ m nominal pore size). This step ensured a comprehensive examination of both nutrient dynamics and the
203 isotopic composition of the particulate pool in the incubated samples. Samples were stored at -20 °C until further analysis.
204 Upon arrival in the lab, the filters were dried at 60 °C and to eliminate particulate inorganic carbon, subsequently subject to
205 acid fuming during which they were exposed to concentrated hydrochloric acid (HCL) vapors overnight in a desiccator. After
206 undergoing acid treatment, the filters were carefully dried, then placed into tin capsules and pelletized for subsequent analysis.
207 The determination of POC and PON, as well as isotopic composition (δ ¹³C POC / δ ¹⁵N PON), was carried out using an
208 elemental analyzer (Flash EA, ThermoFisher, USA) connected to a mass spectrometer (Delta V Advantage Isotope Ratio MS,
209 ThermoFisher, USA) with the ConFlo IV interface. This analytical setup was applied to all filters. These values, derived from
210 triplicate incubation measurements, exhibited no omission of data points or identification of outliers. Final rate calculations for
211 N₂ fixation rates were performed after Mohr et al. (2010) and primary production rates after Slawyk et al. (1977).

Deleted: In the same manner, discrete water samples were obtained using a 10 L Niskin bottle, manually lowered with a hand winch to five distinct depths (Surface, 5, 25, 50, 100 m). These systematic and multifaceted sampling methodologies provide a robust dataset for a comprehensive analysis of the hydrographic conditions in Qeqertarsuaq.

219 **2.3 Molecular methods**

220
221 The filters were flash-frozen in liquid nitrogen, crushed and DNA was extracted using the Qiagen DNA/RNA AllPrep Kit (Qi-
222 agen, Hildesheim, DE), following the procedure outlined by the manufacturer. The concentration and quality of the extracted
223 DNA was assessed spectrophotometrically using a MySpec spectrofluorometer (VWR, Darmstadt, Germany). The prepara-
224 tion of the metagenome library and sequencing were performed by BGI (China). Sequencing libraries were generated using
225 MGIEasy Fast FS DNA Library Prep Set following the manufacturer's protocol. Sequencing was conducted with 2x150bp on
226 a DNBSEQ-G400 platform (MGI). SOAPnuke1.5.5 (Chen et al. (2018)) was used to filter and trim low quality reads and
227 adaptor contaminants from the raw sequence reads, as clean reads. In total, fifteen metagenomic datasets were produced with
228 an average of 9.6G bp per sample.

229 **2.3.1 Metagenomic De Novo assembly, gene prediction, and annotation**

230
231 Megahit v1.2.9 (Li et al. (2015)) was used to assemble clean reads for each dataset with its minimum contig length as 500.
232 Prodigal v2.6.3 (Hyatt et al. (2010)) with the setting of “-p meta” was then used to predict the open reading frames (ORFs) of
233 the assembled contigs. ORFs from all the available datasets were filtered (>100bp), dereplicated and merged into a catalog of
234 non-redundant genes using cd-hit-est (>95 % sequence identity) (Fu et al. (2012)). Salmon v1.10.0 (Patro et al. (2017)) with
235 the “- meta” option was employed to map clean reads of each dataset to the catalog of non-redundant genes and generate the
236 GPM (genes per million reads) abundance. EggNOG mapper v2.1.12 (Cantalapiedra et al. (2021)) was then performed to assign
237 KEGG Orthology (KO) and identify specific functional annotation for the catalog of non-redundant genes. The marker genes,
238 *nifDK* (K02586, K02591 nitrogenase molybdenum-iron protein alpha/beta chain) and *nifH* (K02588, nitrogenase iron protein),
239 were used for the evaluation of microbial potential of N₂ fixation. *RbcL* (K01601, ribulose-bisphosphate carboxylase large
240 chain) and *psbA* (K02703, photosystem II P680 reaction center D1 protein) were selected to evaluate the microbial potential
241 of carbon fixation and photosynthesis, respectively. [The molecular datasets have been deposited with the accession number:](#)
242 [Bioproject PRJNA1133027](#).

243 **3 Results and discussion**

244 **3.1 Hydrographic conditions in Qeqertarsuaq (Disco Bay) and Sullorsuaq (Vaigat) Strait**

245 Disko Bay (Qeqertarsuaq) is located along the west coast of Greenland (Kalaallit Nunaat) at approximately 69 °N (Figure 1),
246 and is strongly influenced by the West Greenland Current (WGC) which is associated with the broader Baffin Bay Polar Waters
247 (BBPW) (Mortensen et al., 2022; Hansen et al., 2012). The WGC does not only significantly shape the hydrographic conditions
248 within the bay but also plays an important role in the larger context of Greenland Ice Sheet melting (Mortensen et al. (2022)).
249 Central to the hydrographic system of the Qeqertarsuaq area is the Jakobshavn Isbræ, which is the most productive glacier in
250 the northern hemisphere and believed to drain about 7 % of the Greenland Ice Sheet and thus contributes substantially to the
251 water influx into the Qeqertarsuaq (Holland et al. (2008)). A predicted increased inflow of warm subsurface water, originating

Formatted: Indent: Left: 0,14 cm, Right: 0,66 cm, Space Before: 0,05 pt

Field Code Changed

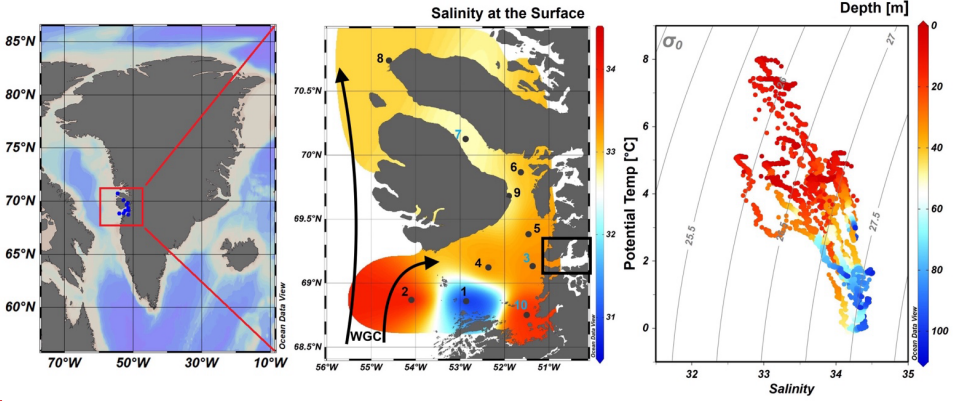
Field Code Changed

Deleted: ,

Deleted: ¶

Formatted: Font: 10 pt

256 from North Atlantic waters, has been suggested to further affect the melting of the Jakobshavn Isbræ and thus adds another
257 layer of complexity to this dynamic system (Holland et al., 2008; Hansen et al., 2012).
258 The hydrographic conditions in Qeqertarsuaq have a significant influence on biological processes, nutrient availability, and the



259
260 **Figure 1.** Map of Greenland (Kalaallit Nunaat) with indication of study area (red box), on the left. Interpolated distribution of Sea Surface
261 Salinity (SSS) values with corresponding isosurface lines and indication of 10 sampled stations (normal stations in black, incubation stations
262 in blue), [black arrows indicate the West Greenland Current \(WGC\)](#) and the black box indicate the location of the Jakobshavn Isbræ, in
263 the middle. Scatterplot of the [potential](#) temperature and salinity for all station data. The plot is used for the identification of the main water
264 masses within the study area. Isopycnals (kg m^{-3}) are depicted in grey lines, on the right. Figures were created in Ocean Data View (ODV)
265 (Schlitzer (2022)).

266 broader marine ecosystem (Munk et al., 2015; Hendry et al., 2019; Schiøtt, 2023).

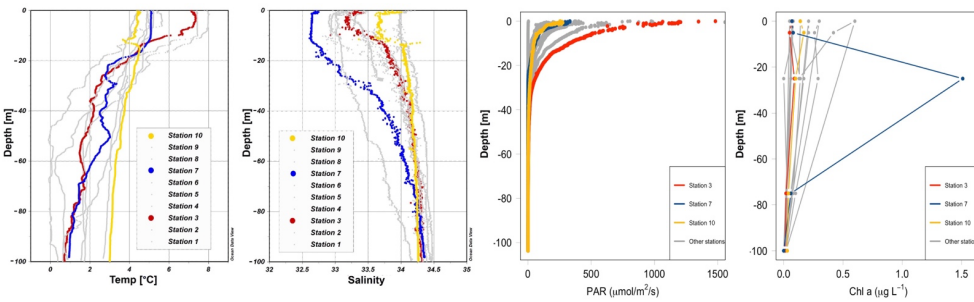
267 During our survey, we found very heterogenous hydrographic conditions at the different stations across Qeqertarsuaq (Fig. 1 &
268 Fig. 2). The three selected stations for N_2 fixation analysis (stations 3, 7, and 10) were strategically chosen to capture the spatial
269 variability of the area. Surface salinity and temperature measurements at these stations indicate the influence of freshwater
270 input. The surface temperature exhibit a range of 4.5 to 8 °C, while surface salinity varies between 31 and 34, as illustrated in
271 Fig. 1. The profiles sampled during our survey extend to a maximum depth of 100 m. Comparison of temperature/salinity (T/S)
272 plots with recent studies suggests the presence of previously described water masses, including Warm Fjord Water (WFjW)
273 and Cold Fjord Water (CFjW) with an overlaying surface glacial meltwater runoff. Those water masses are defined with a
274 density range of $27.20 \leq \sigma_0 \leq 27.31$ but different temperature profiles. Thus water masses can be differentiated by their
275 temperature within the same density range (Gladish et al. (2015)). Other water masses like upper subpolar mode water
276 (uSPMW), deep subpolar mode water (dSPMW) and Baffin Bay polar Water (BBPW) which has been identified in the Disko
277

Deleted: <object>

Deleted: conservative

280
281

Bay (Qeqertarsuaq) before, cannot be identified from this data and may be present in deeper layers (Mortensen et al., 2022; Sherwood et al., 2021; Myers and Ribergaard, 2013; Rysgaard et al., 2020). The temperature and salinity profiles across the 10



282
283
284

285 **Figure 2.** Profiles of temperature (°C), salinity, photosynthetically active radiation (PAR) ($\mu\text{mol}/\text{m}^2/\text{s}$) and Chl *a* (mg m^{-3}) across stations 1 to 286 10 with depth (m). Stations 3, 7, and 10 are highlighted in red, blue, and yellow, respectively, to emphasize incubation stations. Figures were 287 created in Ocean Data View and R-Studio (Schlitzer (2022)).

288

289 stations in the study area show distinct stratification and variability, which is represented through the three incubation stations 290 (highlighted stations 3, 7, and 10 in Fig. 2). They display varying degrees of stratification and mixing, with notable differences 291 in the salinity and temperature profiles. Station 3 and station 7 exhibit clear stratification in both temperature and salinity 292 marked by the presence of thermoclines and haloclines. These features suggest significant freshwater input influenced by local 293 weather conditions and climate dynamics, like surface heat absorption. In contrast, Station 10 exhibits a narrower range of 294 temperature and salinity values throughout the water column compared to Stations 3 and 7, indicating more well-mixed 295 conditions. This uniformity is likely influenced by the regional circulation pattern and partial upwelling (Hansen et al., 2012; 296 Krawczyk et al., 2022). The distinct characteristics observed at station 10, as illustrated in the surface plot (Fig. 1), show an 297 elevated salinity and colder temperatures compared

298

299 to the other stations. This feature suggests upwelling of deeper waters along the shallower shelf, likely facilitated by the local 300 seafloor topography. Specifically, the seafloor shallowing off the coast of Station 10 may act as a barrier, disrupting typical 301 circulation and forcing deeper, saltier, and colder waters to the surface. This pattern aligns with previous studies that describe 302 similar mechanisms in the region (Krawczyk et al. (2022)). Their description of the bathymetry in Qeqertarsuaq, featuring 303 depths ranging from ca. 50 to 900 m, suggests its impact on turbulent circulation patterns, leading to the mixing of different 304 water masses. Evident variability in oceanographic conditions that can be observed throughout the study area occurs particularly 305 along characteristic topographical features like steep slopes, canyons, and shallower areas. The summer melting of sea ice and 306 glaciers introduces freshwater influxes that create distinct vertical and horizontal gradients in salinity and temperature in the 307 Qeqertarsuaq area Hansen et al. (2012). Additionally, the accelerated melting of the Jakobshavn Isbraæ, influenced by the

Deleted: <object>

Formatted: Indent: Left: 0,14 cm, Right: 0,66 cm

Deleted: In contrast station 10 shows more homogeneous salinity and temperature throughout the water column, indicative of well-mixed conditions.

Deleted: ¶

Formatted: Indent: Left: 0 cm

Deleted: likely influenced by the seafloor shallowing off the coast of station 10, which acts as a barrier and disrupts typical circulation. The presence of water masses forced to the surface due to this topographical feature may explain the observed properties at station 10. Furthermore, the variability in temperature and salinity conditions between stations, particularly in relation to topography, aligns with the findings of

320 warmer inflow from the West Greenland Intermediate Current (WGIC), further alters the hydrographic conditions. Recent
321 observations indicate significant warming and shoaling of the WGIC, potentially enabling it to overcome the sill separating the
322 Illulissat Fjord from the Qeqertarsuaq area (Hansen et al., 2012; Holland et al., 2008; Myers and Ribergaard, 2013). This shift
323 intensifies glacier melting, driving substantial changes in the local ecological dynamics (Ardyna et al., 2014; Arrigo et al., 2008;
324 Bhatia et al., 2013).

325 **3.2 Elevated N₂ fixation rates might play a role in nutrient dynamics and bloom development**

326
327 We quantified N₂ fixation rates within the waters of Qeqertarsuaq, spanning from the surface to a depth of 50 m (Table 1). The
328 rates ranged from 0.16 to 2.71 nmol N L⁻¹ d⁻¹ with all rates surpassing the detection limit. Our findings represent rates at the
329 upper range of those observed in the Arctic Ocean. Previous measurements in the region have been limited, with only one
330 study in Baffin Bay by Blais et al. (2012), reporting rates of 0.02 nmol N L⁻¹ d⁻¹, which are 1-2 orders of magnitude lower than
331 our observations. Moreover, Sipler et al. (2017), reported rates in the coastal Chukchi Sea, with average values of 7.7 nmol N
332 L⁻¹ d⁻¹. These values currently represent some of the highest rates measured in Arctic shelf environments. Compared to these,
333 our highest measured rate (2.71 nmol N L⁻¹ d⁻¹) is slower, but still substantial, particularly considering the more Atlantic-
334 influenced location of our study site. Sipler et al. (2017) also noted that a significant fraction of diazotrophs were <3 µm in
335 size, suggesting that small unicellular diazotrophs play a dominant role in Arctic nitrogen fixation. Altogether, our data
336 contribute to the growing evidence that N₂ fixation is a widespread and potentially significant nitrogen source across various
337 Arctic regions. Simultaneous primary production rate measurements ranged from 0.07 to 3.79 µmol N L⁻¹ d⁻¹, with the highest
338 rates observed at station 7 and generally higher values in the surface layers. Employing Redfield stoichiometry, the measured
339 N₂ fixation rates accounted for 0.47 to 2.6 % (averaging 1.57 %) of primary production at our stations. The modest contribution
340 to primary production suggests that N₂ fixation ~~does~~ not exert a substantial influence on the productivity of these waters during
341 the time of the sampling. Rather, our N₂ fixation rates suggest primary production to depend mostly on additional nitrogen
342 sources including regenerated, meltwater or land based sources.

343 The N:P ratio, calculated as DIN to DIP, indicates a deficit in N for primary production based on Redfield stoichiometry (Fig.
344 3). This aligns with findings presented by Jensen et al. (1999) and Tremblay and Gagnon (2009), who observed a similar nitrogen
345 limitation in this region. Such biogeochemical conditions would be expected to generate a niche for N₂ fixing organisms
346 (Sohm et al. (2011)). While N₂ fixation did not chiefly sustain primary production during our sampling campaign, we hypothesize that N₂ fixation ~~has the potential to~~ play a role in bloom dynamics. As nitrogen availability decreases,
347 during a bloom, it may provide a niche for N₂ fixation, potentially extending the productive period of the bloom (Reeder et al.
348 (2021)). Satellite data indicates that a fall bloom began in early August, following the annual spring bloom, as described by
349 Ardyna et al. (2014). This double bloom situation may be driven by increased melting and the subsequent input of bioavailable
350 nutrients and iron (Fe) from meltwater runoff (Arrigo et al., 2017; Hopwood et al., 2016; Bhatia et al., 2013). The meltwater
351 from the Greenland Ice Sheet is a significant source of Fe (Bhatia et al., 2013; Hawkins et al., 2015, 2014), which is a limiting
352 factor especially for diazotrophs (Sohm et al. (2011)). Consequently, it is possible that nutrients and Fe from the Isbræ glacier
353

← Formatted: Space Before: 0,05 pt, Line spacing: Multiple 1,44 li

Deleted: Compared to other European Arctic waters, our rates at the surface and at 25 m water depth fall within the reported range for Arctic estuarine stations (1.04 to 1.87 nmol N L⁻¹ d⁻¹, (SD ± 0.76 to 1.19) and marine stations (0.11 to 0.12 nmol N L⁻¹ d⁻¹, (SD ± 0.09 to 0.09) (Blais et al. (2012)). However, we observed some of the highest rates reported so far, particularly at the surface.

Deleted: relatively

Deleted: may

Formatted: Right: 0,66 cm, Space Before: 0,1 pt

Deleted: the relatively high

Deleted: rates observed

Deleted: may

Deleted: 1

Formatted: Indent: Left: 0 cm

369 introduced into the Qeqertarsuaq are promoting a bloom and further provide a niche for diazotrophs to thrive (Arrigo et al.
370 (2017)).

371
372
373 **Table 1.** N_2 fixation (nmol N L⁻¹ d⁻¹), standard deviation (SD), primary productivity (PP; $\mu\text{mol C L}^{-1} \text{d}^{-1}$), SD, percentage of estimated new
374 primary productivity (% New PP) sustained by N_2 fixation, dissolved inorganic nitrogen compounds (NO_x), phosphorus (PO₄), and the molar
375 nitrogen-to-phosphorus ratio (N:P) at stations 3, 7, and 10.

Station (no.)	Depth (m)	N ₂ fixation (nmol N L ⁻¹ d ⁻¹)	SD (\pm)	Primary Productivity ($\mu\text{mol C L}^{-1} \text{d}^{-1}$)	SD (\pm)	% New PP (%)	NO _x ($\mu\text{mol L}^{-1} \text{d}^{-1}$)	PO ₄ ($\mu\text{mol L}^{-1} \text{d}^{-1}$)
3	0	1.20	0.21	0.466	0.08	1.71	0	0
3	25	1.88	0.11	0.588	0.04	2.11	0	0.70
3	50	0.29	0.01	0.209	0.00	0.91	0.33	1.48
7	0	2.49	0.44	0.63	0.20	2.60	0	0
7	25	2.71	0.22	3.79	2.45	0.47	0	0.45
7	50	0.53	0.24	0.33	0.36	1.08	0	0.97
10	0	1.48	0.12	0.74	0.15	1.33	0	0
10	25	0.31	0.01	0.29	0.07	0.73	0	0
10	50	0.16	0	0.07	0.07	1.40	0	0

377 A near-Redfield stoichiometry in POC:PON indicates that the particulate organic matter (POM) is freshly derived from an
378 ongoing phytoplankton bloom, as phytoplankton generally assimilate carbon and nitrogen in relatively consistent proportions
379 during active growth. In contrast, deviations from the Redfield ratio (e.g., elevated C:N or C:P) typically indicate microbial
380 degradation and preferential remineralization of nitrogen and phosphorus (Redfield 1934; Geider and La Roche 2002; Sterner
381 and Elser 2017). The absence of NO_x and the observed low N:P ratios suggest that nitrogen from earlier bloom phases has
382 been largely depleted, potentially creating a niche for N_2 fixation as a supplementary nitrogen source. The onset and
383 development of the bloom would be expected to lead to high nitrogen demands and intense competition for nitrogen sources.
384 Notably, despite the apparent balance in the POM pool, the N:P ratio indicates strong nitrogen depletion and nutrient exhaustion
385 within the ecosystem. This deficiency can be partly alleviated by N_2 fixation, providing possibly increasing amounts of nitrogen
386 over the course of the bloom. Moreover, DIP is generally limited in the environment (Table 1); however, some organisms may
387 still access it through luxury phosphorus uptake, storing excess phosphate when it is sporadically available. A recent study
388 by Laso Perez et al. (2024) documented changes in microbial community composition during an Arctic bloom, focusing on
389 nitrogen cycling. They observed a shift from chemolithotrophic to heterotrophic organisms throughout the summer bloom and
390 noted increased activity to compete for various nitrogen sources. However, no *nif/H* gene copies, indicative of nitrogen-fixing

391 Deleted: compunds

Deleted: 3

Formatted: Line spacing: Multiple 1.46 li

Deleted: bloom. However, the absence of NO_x (with the exception of one station) and the observed low N:P ratios suggest that any available nitrogen from earlier phases of the bloom has likely been depleted. This could create a niche for N_2 fixation as a supplementary nitrogen source, potentially supporting continued production during this stage of the bloom.

Moved (insertion) [2]

Deleted: ¶

Field Code Changed

Field Code Changed

organisms, were found in their dataset based on metagenome-assembled genomes (MAGs). This is not unexpected due to the classically low abundance of diazotrophs in marine microbial communities which has often been described (Turk-Kubo et al., 2015; Farnelid et al., 2019). Given the high productivity and metabolic activity observed in Qeqertarsuaq during a similar bloom period, the detected diazotrophs (Section 3.3) may play a more significant role than previously thought. Across the 10 stations there is considerable variability in POC and PON concentrations (Fig. 3). PON concentrations range from 0.0 $\mu\text{mol N L}^{-1}$ to 3.48 $\mu\text{mol N L}^{-1}$ (n=124), while POC concentrations range from 2.7 $\mu\text{mol C L}^{-1}$ to 27.2 $\mu\text{mol C L}^{-1}$ (n=144). The highest concentrations for both PON and POC were observed at station 7 at a depth of 25 m and coincide with the highest reported N_2 fixation rate (Figure Appendix A2 & A3). Generally, POC and PON concentrations decrease with depth, peaking at the deep chl *a* maximum (DCM), identified between 15 to 30 m across all stations. The DCM was identified based on measured chl *a* concentrations and previous descriptions in the region (Fox and Walker, 2022; Jensen et al., 1999). The variability in chl *a* concentrations indicates differences in phytoplankton abundance among the stations, with concentrations ranging between 0 to 0.42 mg m^{-3} . Excluding station 7, which exhibited the highest chl *a* concentration at the DCM (1.51 mg m^{-3}). While Tang et al. (2019) found that N_2 fixation measurements strongly correlated to satellite estimates of chl *a* concentrations, our results did not show a statistically significant correlation between nitrogen fixation rates and chl *a* concentrations overall (Figures A2 & A3). However, as noted, Station 7 at 25 m represents a unique case. The elevated concentration of chl *a* at this station likely resulted from a local phytoplankton bloom induced by meltwater outflow from the Isbræ glacier and sea ice melting, which may help explain the observed nitrogen fixation rates (Arrigo et al., 2017; Wang et al., 2014). This study's findings are in agreement with prior reports of analogous blooms occurring in the region (Fox and Walker, 2022; Jensen et al., 1999).

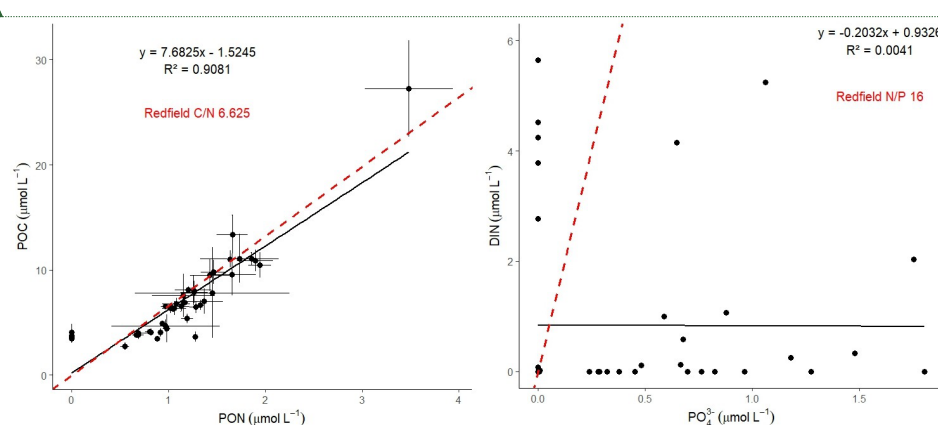


Figure 3. The POC/PON and DIN/DIP ratios at all 10 stations. The red line represents the Redfield ratios of POC/PON (106:16) and DIN/DIP (16:1).

Field Code Changed
Deleted: ¶

Moved up [2]: by Laso Perez et al. (2024) documented changes in microbial community composition during an Arctic bloom, focusing on nitrogen cycling. They observed a shift from chemolithotrophic to heterotrophic organisms throughout the summer bloom and noted increased activity to compete for various nitrogen sources. However, no *nifH* gene copies, indicative of nitrogen-fixing organisms, were found in their dataset based on metagenome-assembled genomes (MAGs). This is not unexpected due to the classically low abundance of diazotrophs in marine microbial communities which has often been described (Turk-Kubo et al., 2015; Farnelid et al., 2019). Given the high productivity and metabolic activity observed in Qeqertarsuaq during a similar bloom period, the detected diazotrophs (Section 3.3) may play a more significant role than previously thought. Across the 10 stations there is considerable variability in POC and PON concentrations (Fig. 3). PON concentrations range from 0.0 $\mu\text{mol N L}^{-1}$ to 3.48 $\mu\text{mol N L}^{-1}$ (n=124), while POC concentrations range from 2.7 $\mu\text{mol C L}^{-1}$ to 27.2 $\mu\text{mol C L}^{-1}$ (n=144). The highest concentrations for both PON and POC were observed at station 7 at a depth of 25 m and coincide with the highest reported N_2 fixation rate (Figure Appendix A2 & A3). Generally, POC and PON concentrations decrease with depth, peaking at the deep chl *a* maximum (DCM), identified between 15 to 30 m across all stations. The DCM was identified based on measured chl *a* concentrations and previous descriptions in the region (Fox and Walker, 2022; Jensen et al., 1999). The variability in chl *a* concentrations indicates differences in phytoplankton abundance among the stations, with concentrations ranging between 0 to 0.42 mg m^{-3} . Excluding station 7, which exhibited the highest chl *a* concentration at the DCM (1.51 mg m^{-3}). While Tang et al. (2019) found that N_2 fixation measurements strongly correlated to satellite estimates of chl *a* concentrations, our results did not show a statistically significant correlation between nitrogen fixation rates and chl *a* concentrations overall (Figures A2 & A3). However, as noted, Station 7 at 25 m represents a unique case. The elevated concentration of chl *a* at this station likely resulted from a local phytoplankton bloom induced by meltwater outflow from the Isbræ glacier and sea ice melting, which may help explain the observed nitrogen fixation rates (Arrigo et al., 2017; Wang et al., 2014). This study's findings are in agreement with prior reports of analogous blooms occurring in the region (Fox and Walker, 2022; Jensen et al., 1999).

448
449
450 **3.3 Potential Contribution of UCYN-A to Nitrogen Fixation During a Diatom Bloom: Insights and Uncertainties**

451 In our metagenomic analysis, we filtered the *nifH*, *nifD*, *nifK* genes, which code for the nitrogenase enzyme responsible for
452 catalyzing N₂ fixation. We could identify sequences related to UCYN-A, which dominated the sequence pool of diazotrophs,
453 particularly in the upper water masses (0 to 5 m) (Fig. 4). UCYN-A, a unicellular cyanobacterial symbiont, has a cosmopolitan
454 distribution and is thought to substantially contribute to global N₂ fixation, as documented by (Martínez-Pérez et al., 2016;
455 Tang et al., 2019). This conclusion is based on our metagenomic analysis, in which we set a sequence identity threshold of
456 95% for both *nif* and photosystem genes. Notably, we only recovered sequences related to UCYN-A within our *nif* sequence
457 pool, suggesting its predominance among detected diazotrophs. However, metagenomic approaches may underestimate overall
458 diazotroph diversity, and we cannot fully exclude the presence of other, less abundant diazotrophs that may have been missed
459 using this method. While UCYN-A was primarily detected in surface waters, we also observed relatively high *nifK* values at
460 S3 100m, an unusual finding given that UCYN-A is typically constrained to the euphotic zone. Previous studies have
461 predominantly reported UCYN-A in surface waters; for instance Harding et al. (2018) and Shiozaki et al. (2017) detected
462 UCYN-A exclusively in the upper layers of the Arctic Ocean. Additionally, Shiozaki et al. (2020) found UCYN-A2 at depths
463 extending to the 0.1% light level but not below 66 m in the Chukchi Sea. The detection of UCYN-A at 100 m in our study
464 suggests that alternative mechanisms, such as particle association, vertical transport, or local environmental conditions, may
465 facilitate its presence at depth. This warrants further investigation into the potential processes enabling its occurrence below
466 the euphotic zone.

467 Due to the lack of genes such as those encoding Photosystem II and Rubisco, UCYN-A plays a significant role within the host
468 cell and participates in fundamental cellular processes. Consequently it has evolved to become a closely integrated component
469 of the host cell. Very recent findings demonstrate that UCYN-A imports proteins encoded by the host genome and has been
470 described as an early form of N₂ fixing organelle termed a "Nitroplast" (Coale et al. (2024)).

471 Previous investigations document that they are critical for primary production, supplying up to 85% of the fixed nitrogen to their
472 haptophyte host (Martínez-Pérez et al. (2016)). In addition to its high contribution to primary production, studies have shown
473 that UCYN-A in high latitude waters fix similar amounts of N₂ per cell as in the tropical Atlantic Ocean, even in nitrogen-
474 replete waters (Harding et al., 2018; Shiozaki et al., 2020; Martínez-Pérez et al., 2016; Krupke et al., 2015; Mills et al., 2020).
475 However, estimating their contribution to N₂ fixation in our study is challenging, particularly since we detected cyanobacteria
476 only at the surface but observe significant N₂ fixation rates below 5 m. The diazotrophic community is often underrepresented
477 in metagenomic datasets due to the low abundance of nitrogenase gene copies, implying our data does not present a complete
478 picture. We suspect a more diverse diazotrophic community exists, with UCYN-A being a significant contributor to N₂ fixation
479 in Arctic waters. However, the exact proportion of its contribution requires further investigation.

480 The contribution of N₂ fixation to carbon fixation (as percent of PP) is relatively low, at the time of our study. We identified
481 genes such as *rbcL*, which encodes Rubisco, a key enzyme in the carbon fixation pathway and *psbA*, a gene encoding

482
483
484
485
486
487
488
489
490
491
492
493
494
495
496
497
498
499
500
501
502
503
504
505
506
507
508
509
510
511
512
513
514
515
516
517
518
519
520
521
522
523
524
525
526
527
528
529
530
531
532
533
534
535
536
537
538
539
540
541
542
543
544
545
546
547
548
549
550
551
552
553
554
555
556
557
558
559
560
561
562
563
564
565
566
567
568
569
570
571
572
573
574
575
576
577
578
579
580
581
582
583
584
585
586
587
588
589
590
591
592
593
594
595
596
597
598
599
600
601
602
603
604
605
606
607
608
609
610
611
612
613
614
615
616
617
618
619
620
621
622
623
624
625
626
627
628
629
630
631
632
633
634
635
636
637
638
639
640
641
642
643
644
645
646
647
648
649
650
651
652
653
654
655
656
657
658
659
660
661
662
663
664
665
666
667
668
669
670
671
672
673
674
675
676
677
678
679
680
681
682
683
684
685
686
687
688
689
690
691
692
693
694
695
696
697
698
699
700
701
702
703
704
705
706
707
708
709
710
711
712
713
714
715
716
717
718
719
720
721
722
723
724
725
726
727
728
729
730
731
732
733
734
735
736
737
738
739
740
741
742
743
744
745
746
747
748
749
750
751
752
753
754
755
756
757
758
759
760
761
762
763
764
765
766
767
768
769
770
771
772
773
774
775
776
777
778
779
780
781
782
783
784
785
786
787
788
789
790
791
792
793
794
795
796
797
798
799
800
801
802
803
804
805
806
807
808
809
810
811
812
813
814
815
816
817
818
819
820
821
822
823
824
825
826
827
828
829
830
831
832
833
834
835
836
837
838
839
840
841
842
843
844
845
846
847
848
849
850
851
852
853
854
855
856
857
858
859
860
861
862
863
864
865
866
867
868
869
870
871
872
873
874
875
876
877
878
879
880
881
882
883
884
885
886
887
888
889
890
891
892
893
894
895
896
897
898
899
900
901
902
903
904
905
906
907
908
909
910
911
912
913
914
915
916
917
918
919
920
921
922
923
924
925
926
927
928
929
930
931
932
933
934
935
936
937
938
939
940
941
942
943
944
945
946
947
948
949
950
951
952
953
954
955
956
957
958
959
960
961
962
963
964
965
966
967
968
969
970
971
972
973
974
975
976
977
978
979
980
981
982
983
984
985
986
987
988
989
990
991
992
993
994
995
996
997
998
999
1000
1001
1002
1003
1004
1005
1006
1007
1008
1009
10010
10011
10012
10013
10014
10015
10016
10017
10018
10019
10020
10021
10022
10023
10024
10025
10026
10027
10028
10029
10030
10031
10032
10033
10034
10035
10036
10037
10038
10039
10040
10041
10042
10043
10044
10045
10046
10047
10048
10049
10050
10051
10052
10053
10054
10055
10056
10057
10058
10059
10060
10061
10062
10063
10064
10065
10066
10067
10068
10069
10070
10071
10072
10073
10074
10075
10076
10077
10078
10079
10080
10081
10082
10083
10084
10085
10086
10087
10088
10089
10090
10091
10092
10093
10094
10095
10096
10097
10098
10099
100100
100101
100102
100103
100104
100105
100106
100107
100108
100109
100110
100111
100112
100113
100114
100115
100116
100117
100118
100119
100120
100121
100122
100123
100124
100125
100126
100127
100128
100129
100130
100131
100132
100133
100134
100135
100136
100137
100138
100139
100140
100141
100142
100143
100144
100145
100146
100147
100148
100149
100150
100151
100152
100153
100154
100155
100156
100157
100158
100159
100160
100161
100162
100163
100164
100165
100166
100167
100168
100169
100170
100171
100172
100173
100174
100175
100176
100177
100178
100179
100180
100181
100182
100183
100184
100185
100186
100187
100188
100189
100190
100191
100192
100193
100194
100195
100196
100197
100198
100199
100200
100201
100202
100203
100204
100205
100206
100207
100208
100209
100210
100211
100212
100213
100214
100215
100216
100217
100218
100219
100220
100221
100222
100223
100224
100225
100226
100227
100228
100229
100230
100231
100232
100233
100234
100235
100236
100237
100238
100239
100240
100241
100242
100243
100244
100245
100246
100247
100248
100249
100250
100251
100252
100253
100254
100255
100256
100257
100258
100259
100260
100261
100262
100263
100264
100265
100266
100267
100268
100269
100270
100271
100272
100273
100274
100275
100276
100277
100278
100279
100280
100281
100282
100283
100284
100285
100286
100287
100288
100289
100290
100291
100292
100293
100294
100295
100296
100297
100298
100299
100300
100301
100302
100303
100304
100305
100306
100307
100308
100309
100310
100311
100312
100313
100314
100315
100316
100317
100318
100319
100320
100321
100322
100323
100324
100325
100326
100327
100328
100329
100330
100331
100332
100333
100334
100335
100336
100337
100338
100339
100340
100341
100342
100343
100344
100345
100346
100347
100348
100349
100350
100351
100352
100353
100354
100355
100356
100357
100358
100359
100360
100361
100362
100363
100364
100365
100366
100367
100368
100369
100370
100371
100372
100373
100374
100375
100376
100377
100378
100379
100380
100381
100382
100383
100384
100385
100386
100387
100388
100389
100390
100391
100392
100393
100394
100395
100396
100397
100398
100399
100400
100401
100402
100403
100404
100405
100406
100407
100408
100409
100410
100411
100412
100413
100414
100415
100416
100417
100418
100419
100420
100421
100422
100423
100424
100425
100426
100427
100428
100429
100430
100431
100432
100433
100434
100435
100436
100437
100438
100439
100440
100441
100442
100443
100444
100445
100446
100447
100448
100449
100450
100451
100452
100453
100454
100455
100456
100457
100458
100459
100460
100461
100462
100463
100464
100465
100466
100467
100468
100469
100470
100471
100472
100473
100474
100475
100476
100477
100478
100479
100480
100481
100482
100483
100484
100485
100486
100487
100488
100489
100490
100491
100492
100493
100494
100495
100496
100497
100498
100499
100500
100501
100502
100503
100504
100505
100506
100507
100508
100509
100510
100511
100512
100513
100514
100515
100516
100517
100518
100519
100520
100521
100522
100523
100524
100525
100526
100527
100528
100529
100530
100531
100532
100533
100534
100535
100536
100537
100538
100539
100540
100541
100542
100543
100544
100545
100546
100547
100548
100549
100550
100551
100552
100553
100554
100555
100556
100557
100558
100559
100560
100561
100562
100563
100564
100565
100566
100567
100568
100569
100570
100571
100572
100573
100574
100575
100576
100577
100578
100579
100580
100581
100582
100583
100584
100585
100586
100587
100588
100589
100590
100591
100592
100593
100594
100595
100596
100597
100598
100599
100600
100601
100602
100603
100604
100605
100606
100607
100608
100609
100610
100611
100612
100613
100614
100615
100616
100617
100618
100619
100620
100621
100622
100623
100624
100625
100626
100627
100628
100629
100630
100631
100632
100633
100634
100635
100636
100637
100638
100639
100640
100641
100642
100643
100644
100645
100646
100647
100648
100649
100650
100651
100652
100653
100654
100655
100656
100657
100658
100659
100660
100661
100662
100663
100664
100665
100666
100667
100668
100669
100670
100671
100672
100673
100674
100675
100676
100677
100678
100679
100680
100681
100682
100683
100684
100685
100686
100687
100688
100689
100690
100691
100692
100693
100694
100695
100696
100697
100698
100699
100700
100701
100702
100703
100704
100705
100706
100707
100708
100709
100710
100711
100712
100713
100714
100715
100716
100717
100718
100719
100720
100721
100722
100723
100724
100725
100726
100727
100728
100729
100730
100731
100732
100733
100734
100735
100736
100737
100738
100739
100740
100741
100742
100743
100744
100745
100746
100747
100748
100749
100750
100751
100752
100753
100754
100755
100756
100757
100758
100759
100760
100761
100762
100763
100764
100765
100766
100767
100768
100769
100770
100771
100772
100773
100774
100775
100776
100777
100778
100779
100780
100781
100782
100783
100784
100785
100786
100787
100788
100789
100790
100791
100792
100793
100794
100795
100796
100797
100798
100799
100800
100801
100802
100803
100804
100805
100806
100807
100808
100809
100810
100811
100812
100813
100814
100815
100816
100817
100818
100819
100820
100821
100822
100823
100824
100825
100826
100827
100828
100829
100830
100831
100832
100833
100834
100835
100836
100837
100838
100839
100840
100841
100842
100843
100844
100845
100846
100847
100848
100849
100850
100851
100852
100853
100854
100855
100856
100857
100858
100859
100860
100861
100862
100863
100864
100865
100866
100867
100868
100869
100870
100871
100872
100873
100874
100875
100876
100877
100878
100879
100880
100881
100882
100883
100884
100885
100886
100887
100888
100889
100890
100891
100892
100893
100894
100895
100896
100897
100898
100899
100900
100901
100902
100903
100904
100905
100906
100907
100908
100909
100910
100911
100912
100913
100914
100915
100916
100917
100918
100919
100920
100921
100922
100923
100924
100925
100926
100927
100928
100929
100930
100931
100932
100933
100934
100935
100936
100937
100938
100939
100940
100941
100942
100943
100944
100945
100946
100947
100948
100949
100950
100951
100952
100953
100954
100955
100956
100957
100958
100959
100960
100961
100962
100963
100964
100965
100966
100967
100968
100969
100970
100971
100972
100973
100974
100975
100976
100977
100978
100979
100980
100981
100982
100983
100984
100985
100986
100987
100988
100989
100990
100991
100992
100993
100994
100995
100996
100997
100998
100999
100100
100101
100102
100103
100104
100105
100106
100107
100108
100109
100110
100111
100112
100113
100114
100115

515 Photosystem II, involved in light-driven electron transfer in photosynthesis, in our metagenomic dataset. The gene *rbcL* (for the
516 carbon fixation pathway) and the gene *psbA* (for primary producers) were used to track the community of photosynthetic primary
517 producers in our metagenomic dataset. At station 7, elevated carbon fixation rates are correlated with high diatom
518 (*Bacillariophyta*) abundance and increased chl *a* concentration (Fig. 4), suggesting the onset of a bloom, which is also
519 observable via satellite images (Appendix A1). We hypothesize that meltwater, carrying elevated nutrient and trace metal
520 concentrations, was rapidly transported away from the glacier through the Vaigat Strait by strong winds, leading to increased
521 productivity, as previously described by Fox and Walker (2022) & Jensen et al. (1999). The elevated diatom abundance and
522 primary production rates at station 7 coincide with the highest N₂ fixation rates, which could possibly point toward a possible
523 diatom-diazotroph symbiosis (Foster et al., 2022, 2011; Schvarcz et al., 2022). However, we did not detect a clear diazotrophic
524 signal directly associated with the diatoms in our metagenomic dataset, which might be due to generally underrepresentation of
525 diazotrophs in metagenomes due to low abundance or low sequencing coverage. To investigate this further, we examined
526 the taxonomic composition of *Bacillariophyta* at higher resolution. Among the various abundant diatom genera,
527 *Rhizosolenia* and *Chaetoceros* have been identified as symbiosis with diazotrophs (Grosse, et al., 2010; Foster, et al.,
528 2010), representing less than 6% or 15% of *Bacillariophyta*, based on *rbcL* or *psbA*, respectively (Figure Appendix A4).
529 Although we underestimate diazotrophs to an extent, the presence of certain diatom-diazotroph symbiosis could help
530 explain the high nitrogen fixation rates in the diatom bloom to a certain degree. Compilation of *nif* sequences identified
531 from this study as well as homologous from their NCBI top hit were added in Table S1. However, we cannot tell if the
532 diazotrophs belong to UCYN-A1 or UCYN-A2, or UCYN-A3. Based on the Pierella Karlusich et al. (2021), they
533 generated clonal *nifH* sequences from Tara Oceans, which the length of *nifH* sequences is much shorter than the two
534 *nifH* sequences we generated in our study. Also, the available UCYN-A2 or UCYN-A3 *nifH* sequences from NCBI were
535 shorter than the two *nifH* sequences we generated. Therefore, it would be not accurate to assign the *nifH* sequences to
536 either group under UCYN-A. Furthermore, not much information is available regarding the different groups of UCYN-
537 A using marker genes of *nifD* and *nifK*.
538

Deleted: s

Deleted: However,

Deleted: ny relevant

Deleted: group

Deleted: observed

Deleted: their absence or due to the

Deleted: .

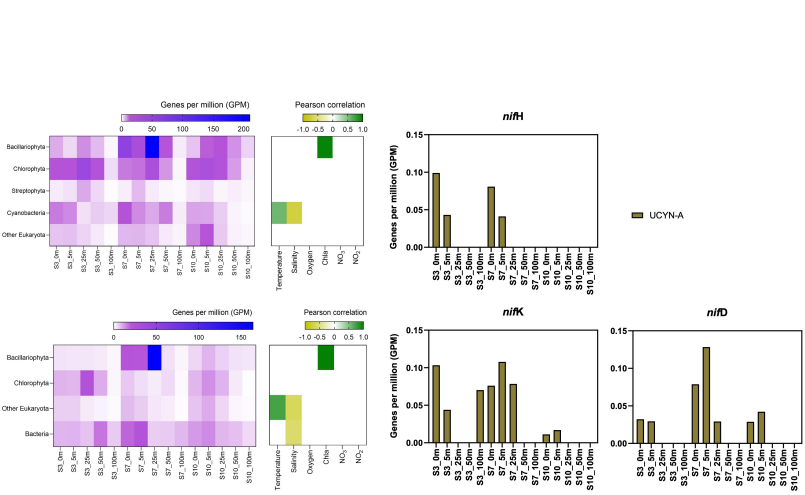
Formatted: Font: Italic

Moved (insertion) [1]

Deleted: Therefore, we can only assume that such a symbiosis explains the elevated rates. Additional molecular approaches would be necessary to enhance our understanding show a more detailed picture of the diazotrophic community.¶

Moved up [1]: a symbiosis explains the elevated rates. Additional molecular approaches would be necessary to enhance our understanding show a more detailed picture of the diazotrophic community.¶

Deleted: ¶



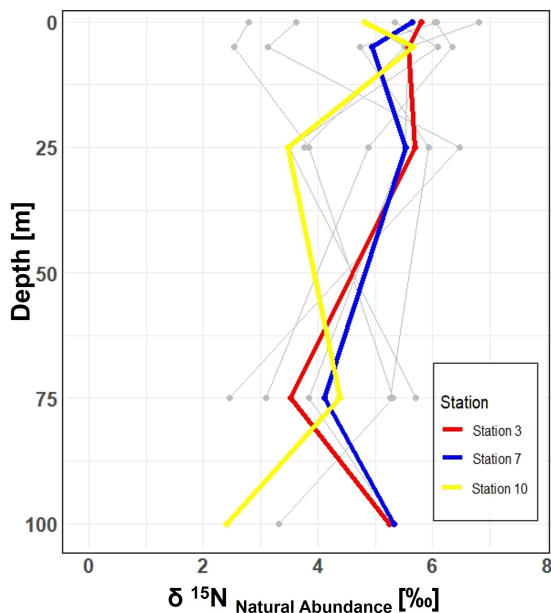
556
557 **Figure 4.** Upper left image: *psbA* with correlation plot. Lower left image: *rbcL* with correlation plot. Right image: *nifH*, *nifD*, *nifK* genes
558 per million reads in the metagenomic datasets. All figures display molecular data from metagenomic dataset for all sampled depth of station
559 3,7,10

560 There is evidence that UCYN-A have a higher Fe demand, with input through meltwater or river runoff potentially being
561 advantageous to those organisms (Shiozaki et al., 2017, 2018; Cheung et al., 2022). Consequently, UCYN-A might play a
562 more critical role in the future with increased Fe-rich meltwater runoff. UCYN-A can potentially fuel primary productivity by
563 supplying nitrogen, especially with increased melting, nutrient inputs, and more light availability due to rising temperatures as-
564 sociated with climate change. This predicted enhancement of primary productivity may contribute to the biological drawdown
565 of CO₂, acting as a negative feedback mechanism. These projections are based on studies forecasting increased temperatures,
566 melting, and resulting biogeochemical changes leading to higher primary productivity. However large uncertainties make pre-
567 dictions very difficult and should be handled with care. Thus we can only hypothesize that UCYN-A might be coupled to these
568 dynamics by providing essential nitrogen.

569 **3.4 $\delta^{15}\text{N}$ Signatures in particulate organic nitrogen show no clear evidence of nitrogen fixation**

570 Stable isotopic composition, expressed using the $\delta^{15}\text{N}$ notation, serve as indicators for understanding nitrogen dynamics
571 because different biogeochemical processes fractionate nitrogen isotopes in distinct ways (Montoya (2008)). However, it is
572 important to keep in mind that the final isotopic signal is a combination of all processes and an accurate distinction between
573 processes cannot be made. N₂ fixation tends to enrich nitrogenous compounds with lighter isotopes, producing OM with
574 isotopic values ranging approximately from -2 to +2 ‰ (Dähnke and Thamdrup (2013)). Upon complete remineralization and
575 oxidation, organic matter contributes to a reduction in the average δ -values in the open ocean (e.g. Montoya et al. (2002);

580 Emeis et al. (2010)). Whereas processes like denitrification and anammox preferentially remove lighter isotopes, leading to
581 enrichment in heavier isotopes and delta values up to -25 ‰.
582



583
584
585 **Figure 5.** Vertical profiles of $\delta^{15}\text{N}$ natural abundance signatures in PON across 10 stations in the study area. Incubation stations 3, 7, and 10
586 are highlighted in red, blue, and yellow, respectively. The figure shows variations in $\delta^{15}\text{N}$ signatures with depth at each station, providing
587 insight into nitrogen cycling in the study area.

588
589 Thus, $\delta^{15}\text{N}$ values help to identify different processes of the nitrogen cycle generally present in a system (Dähne and Tham-
590 drup (2013)). In our study, the $\delta^{15}\text{N}$ values of PON from all 10 stations, range between 2.45 ‰ and 8.30 ‰ within the 0 to
591 100 m depth range, thus do not exhibit a clear signal indicative of N_2 fixation. This suggests that N_2 fixation likely contributes
592 only a certain fraction to export production or that it only started to contribute to isotope fractionation in the bloom dynamic.
593 The composition of OM in the surface ocean is influenced by the nitrogen substrate and the fractionation factor during pho-
594 tosynthesis. When nitrate is depleted in the surface ocean, the isotopic signature of OM produced during photosynthesis will
595 mirror that of the nitrogen substrate. This substrate can originate from either nitrate in the subsurface or N_2 fixation. Notably,

596 nitrate, the primary form of dissolved nitrogen in the open ocean, typically exhibits an average stable isotope value of around
597 5 ‰. No fractionation occurs during photosynthesis because the nitrogen source is entirely taken up in the surface waters
598 (Sigman et al. (2009)). In Qeqertarsuaq, where similar conditions prevail, this suggests that factors other than N₂ fixation ~~are~~
599 influencing the observed δ -values and POM is sustained by nitrogen sources from deeper subsurface waters, as observed in
600 earlier studies (Fox and Walker (2022)).

Deleted: may

Deleted: be

601 In the eastern Baffin Bay waters, Atlantic water masses serve as an important source of nitrate for sustaining primary productivity, which is also reflected in the nitrogen isotopic signature in this study (Sherwood et al. (2021)). The influx of Atlantic
602 waters, characterized by NO₃⁻ values of approximately 5 ‰, closely matches the $\delta^{15}\text{N}$ values of observed PON concentrations
603 in our study. This suggests that Atlantic-derived NO₃⁻ serves as a primary source of new nitrogen to the initial stages of bloom
604 development (Fox and Walker, 2022; Knies, 2022). The mechanisms through which subsurface nitrate reaches the euphotic
605 layer are not well understood. However, potential pathways include vertical migration of phytoplankton and physical mixing.
606 Subsequently, nitrogen undergoes rapid recycling and remineralization processes to meet the system's nitrogen demands
607 (Jensen et al. (1999)).

Deleted: As the bloom progresses and nitrogen from
Atlantic waters is depleted, N₂ fixation may provide an
additional nitrogen source, supporting continued primary
productivity. ...

609 610 4 Conclusion

611 Our study highlights the occurrence of elevated rates of N₂ fixation in Arctic coastal waters, particularly prominent at station 7,
612 where they coincide with high chl *a* values, indicative of heightened productivity. Satellite observations tracing the origin of a
613 bloom near the Isbrae Glacier, subsequently moving through the Vaigat strait, suggest a recurring phenomenon likely triggered
614 by increased nutrient-rich meltwater originating from the glacier. This aligns with previous reports by Jensen et al. (1999) &
615 Fox and Walker (2022), underlining the significance of such events in driving primary productivity in the region. The contribution
616 of N₂ fixation to primary production was low (average 1.57 %) across the stations. Since the demand was high relative to
617 the new nitrogen provided by N₂ fixation, the observed primary production must be sustained by the already present or adequate
618 amount of subsurface supply of NO_x nutrients in the seawater. This is also visible in the isotopic signature of the POM (Fox and
619 Walker, 2022; Sherwood et al., 2021). However, the detected N₂ fixation rates are likely linked to the development of the fresh
620 secondary summer bloom, which could be sustained by high nutrient and Fe availability from melting, potentially leading the
621 system into a nutrient-limited state. The ongoing high demand for nitrogen compounds may suggest an onset to further sustain
622 the bloom, but it remains speculative whether Fe availability definitively contributes to this process. The occurrence of such
623 double blooms has increased by 10 % in the Qeqertarsuaq and even 33 % in the Baffin Bay, with further projected increases
624 moving north from Greenland (Kalaallit Nunaat) waters (Ardyna et al. (2014)). Thus, nutrient demands are likely to increase,
625 and the role of N₂ fixation ~~can~~ become more significant. The diazotrophic community in this study is dominated by UCYN-A in
626 surface waters and may be linked to diatom abundance in deeper layers. This co-occurrence of diatoms and N₂ fixers in the
627 same location is probably due to the co-limitation of similar nutrients, rather than a symbiotic relationship. Thus, this highlights
628 the significant presence of diazotrophs despite their limited representation in datasets. It also highlights the potential for further
629

Deleted: may

discoveries, as existing datasets likely underestimate the full extent of the diazotrophic community (Laso Perez et al., 2024; Shao et al., 2023; Shiozaki et al., 2017, 2023). The reported N_2 fixation rates in the Vaigat strait within the Arctic Ocean are notably higher than those observed in many other oceanic regions, emphasizing that N_2 fixation is an active and significant process in these high-latitude waters. When compared to measured rates across various ocean systems using the ^{15}N approach, the significance of these findings becomes clear. For instance, N_2 fixation rates are sometimes below the detection limit and often relatively low ranging from 0.8 to 4.4 nmol $N\ L^{-1}\ d^{-1}$ (Löscher et al., 2020, 2016; Turk et al., 2011). In contrast, higher rates reach up to 20 nmol $N\ L^{-1}\ d^{-1}$ (Rees et al. (2009)) and sometime exceptional high rates range from 38 to 610 nmol $N\ L^{-1}\ d^{-1}$ (Bonnet et al. (2009)). The Arctic Ocean rates are thus significant in the global context, underscoring the region's role in the global nitrogen cycle and the importance of N_2 fixation in supporting primary productivity in these waters.

These findings highlight the urgent need to understand the interplay between seasonal variations, sea-ice dynamics, and hydrographic conditions in Qeqertarsuaq. As climate change accelerates the melting of the Greenland Ice Sheet at Jakobshavn Isbræ, shifts in hydrodynamic patterns and hydrographic conditions in Qeqertarsuaq are anticipated. The resulting influx of warmer waters could significantly reshape the bay's hydrography, making it crucial to comprehend the coupling of climate-driven changes and oceanic processes in this vital Arctic region. Our study provides key insights into these dynamics and underscores the importance of continued investigation to predict Qeqertarsuaq's future hydrographic state. By detailing the environmental and hydrographic changes, we contribute valuable knowledge to the broader context of N_2 fixation in the Arctic Ocean. Given nitrogen's pivotal role in Arctic ecosystem productivity, it is essential to explore diazotrophs, quantify N_2 fixation, and assess their impact on ecosystem services as climate change progresses.

Appendix A

Field Code Changed
Deleted: ?;

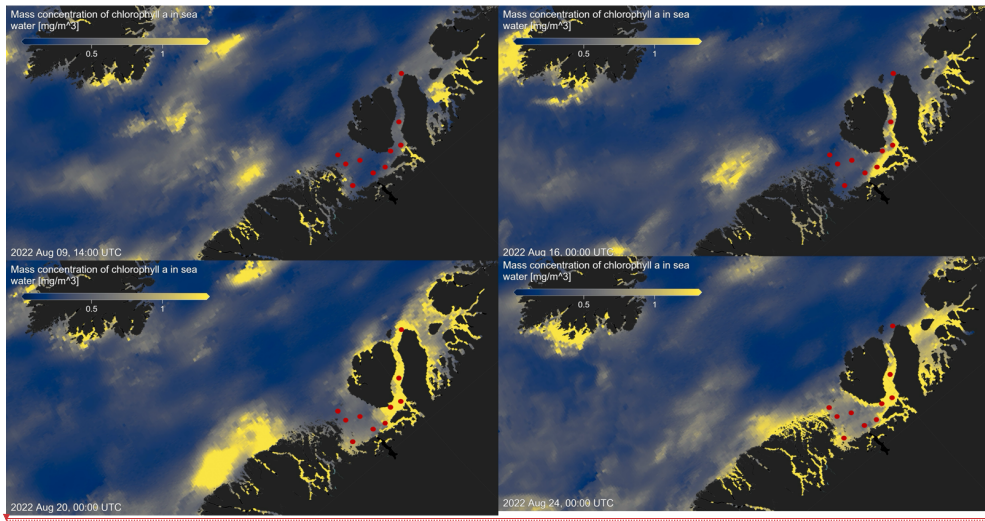
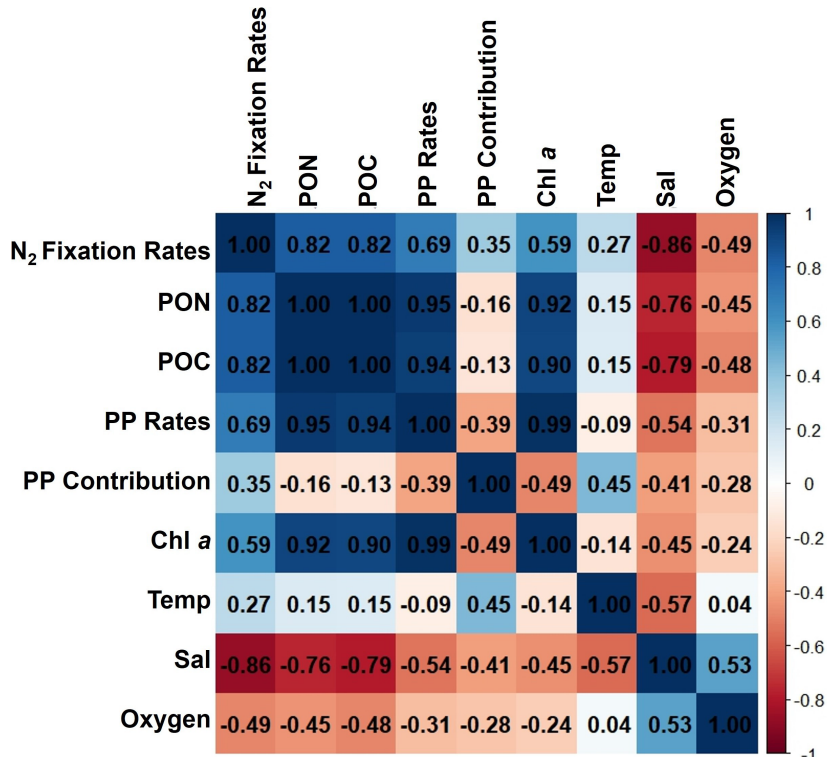


Figure A1. Chlorophyll *a* concentration mg m^{-3} at four time points before, during, and after sea water sampling in August 2022 (sampling stations indicated by red dots), obtained from MODIS-Aqua; <https://giovanni.gsfc.nasa.gov> (Aqua MODIS Global Mapped Chl *a* Data, version R2022.0, DOI:10.5067/AQUA/MODIS/L3M/CHL/2022), 4 km resolution, last access 03 June 2024





664
665
666 **Figure A2.** Correlation matrix of environmental and biological variables. The plot shows the correlation coefficients between the following
667 parameters: N₂ fixation rates, PON, POC, PP rates, the contribution N₂ fixation to PP (PP contribution), Chl a, temperature (Temp), salinity
668 (Sal), and Oxygen. The scale ranges from -1 to 1, where values close to 1 or -1 indicate strong positive or negative correlations, respectively,
669 and values near 0 indicate weak or no correlation. The color intensity represents the strength and direction of the correlations, facilitating the
670 identification of relationships among the variables

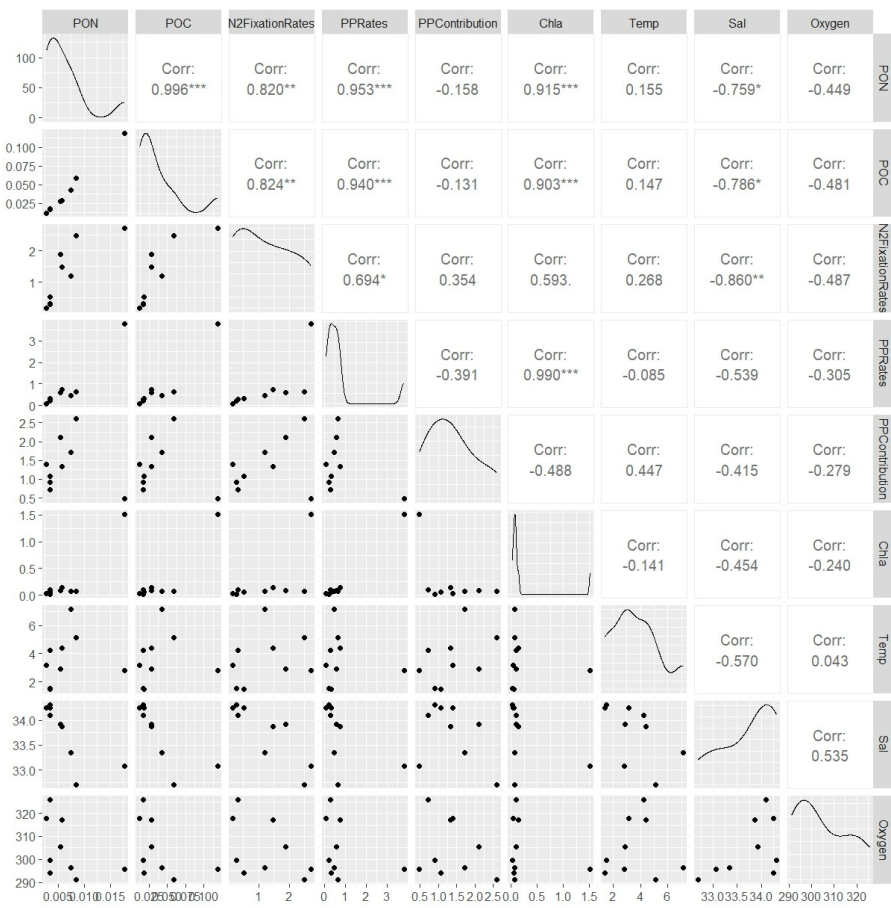


Figure A3. This figure displays a ggpairs plot, showing pairwise relationships and correlations between biological and environmental variables. Pearson correlation coefficients displayed in the upper triangular panel, indicating the strength and significance of linear relationships. Statistical significance levels are indicated by stars (*), where * indicates $p < 0.05$, ** indicates $p < 0.01$ and *** indicates $p < 0.001$

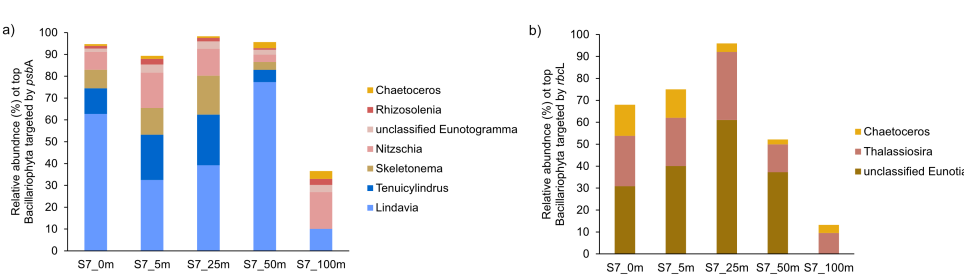


Figure A4. Taxonomic composition of Bacillariophyta at Station 7 based on a) *psbA* and b) *rbcL* marker genes. The figure shows the relative abundance of Bacillariophyta genera detected in the metagenomic dataset, grouped by gene-specific classifications.

Formatted: Keep with next

Formatted: Font: 9 pt, Bold, Font colour: Text 2

Formatted: Font: Not Bold

Deleted: Bioproject PRJNA1133027.

685 *Data availability.* The presented data collected during the cruise will be made accessible on PANGEA. The molecular datasets have been
 686 deposited with the accession number: Bioproject PRJNA1133027.

687
 688
 689 *Author contributions.* IS carried out fieldwork and laboratory work at the University of Southern Denmark, and wrote the majority of the
 690 manuscript. ELP, AM, and EL conducted fieldwork and laboratory work at the University of Southern Denmark. PX performed metagenomic
 691 analysis and created the corresponding graphs. CRL designed the study, provided supervision and guidance throughout the project, and
 692 contributed to the writing and revision of the manuscript. All authors contributed to the conception of the study and participated in the writing
 693 and revision of the manuscript.

694
 695
 696
 697 *Competing interests.* The authors declare that they have no known competing financial interests or personal relationships that could have
 698 appeared to influence the work reported in this paper. One of the authors, CRL, serves as an Associate Editor for Biogeosciences.

700
 701
 702 *Acknowledgements.* This work was supported by the Velux Foundation (grant no.29411 to Carolin R. Löscher) and through the DFF grant
 703 from the the Independent Research Fund Denmark (grant no. 0217-00089B to Lasse Riemann, Carolin R. Löscher and Stig Markager). ELP
 704 was supported by a postdoctoral contract from Danmarks Frie Forskningsfond (DFF, 1026-00428B) at SDU, and by a Marie Skłodowska-
 705 Curie postdoctoral fellowship (HORIZON291 MSCA-2021-PF-01, project number: 101066750) by the European Commission at Princeton
 706 University. We sincerely thank the captain and crew of the P540 during the cruise on the Danish military vessel for their invaluable support and
 707 cooperation at sea. Our gratitude extends to Isaaffik Arctic Gateway for providing the infrastructure and opportunities that made this project
 708 possible. We also acknowledge Zarah Kofoed for her technical support in the laboratory and thank all the Nordceo laboratory technicians for
 709

711 their general assistance.

712 References

713

714 Ardyna, M. and Arrigo, K. R.: Phytoplankton dynamics in a changing Arctic Ocean, *Nature Climate Change*, 10, 892–903, 2020.

715 Ardyna, M., Babin, M., Gosselin, M., Devred, E., Rainville, L., and Tremblay, J.-É.: Recent Arctic Ocean sea ice loss triggers novel fall
716 phytoplankton blooms, *Geophysical Research Letters*, 41, 6207–6212, 2014.

717 Arrigo, K. R. and van Dijken, G. L.: Continued increases in Arctic Ocean primary production, *Progress in oceanography*, 136, 60–70, 2015.

718 Arrigo, K. R., van Dijken, G., and Pabi, S.: Impact of a shrinking Arctic ice cover on marine primary production, *Geophysical Research
719 Letters*, 35, 2008.

720 Arrigo, K. R., van Dijken, G. L., Castelao, R. M., Luo, H., Rennermalm, Å. K., Tedesco, M., Mote, T. L., Oliver, H., and Yager, P. L.:
721 Melting glaciers stimulate large summer phytoplankton blooms in southwest Greenland waters, *Geophysical Research Letters*, 44, 6278–
722 6285, 2017.

723 Bhatia, M. P., Kujawinski, E. B., Das, S. B., Breier, C. F., Henderson, P. B., and Charette, M. A.: Greenland meltwater as a significant and
724 potentially bioavailable source of iron to the ocean, *Nature Geoscience*, 6, 274–278, 2013.

725 Blais, M., Tremblay, J.-É., Jungblut, A. D., Gagnon, J., Martin, J., Thaler, M., and Lovejoy, C.: Nitrogen fixation and identification of
726 potential diazotrophs in the Canadian Arctic, *Global Biogeochemical Cycles*, 26, 2012.

727 Bonnet, S., Biegala, I. C., Dutrieux, P., Slemmons, L. O., and Capone, D. G.: Nitrogen fixation in the western equatorial Pacific: Rates,
728 diazotrophic cyanobacterial size class distribution, and biogeochemical significance, *Global Biogeochemical Cycles*, 23, 2009.

729 Buchanan, P. J., Chase, Z., Matear, R. J., Phipps, S. J., and Bindoff, N. L.: Marine nitrogen fixers mediate a low latitude pathway for
730 atmospheric CO₂ drawdown, *Nature Communications*, 10, 4611, 2019.

731 Cantalapiedra, C. P., Hernández-Plaza, A., Letunic, I., Bork, P., and Huerta-Cepas, J.: eggNOG-mapper v2: functional annotation, orthology
732 assignments, and domain prediction at the metagenomic scale, *Molecular biology and evolution*, 38, 5825–5829, 2021.

733 Capone, D. G. and Carpenter, E. J.: Nitrogen fixation in the marine environment, *Science*, 217, 1140–1142, 1982.

734 Chen, Y., Chen, Y., Shi, C., Huang, Z., Zhang, Y., Li, S., Li, Y., Ye, J., Yu, C., Li, Z., et al.: SOAPnuke: a MapReduce acceleration-supported
735 software for integrated quality control and preprocessing of high-throughput sequencing data, *Gigascience*, 7, gix120, 2018.

736 Cheung, S., Liu, K., Turk-Kubo, K. A., Nishioka, J., Suzuki, K., Landry, M. R., Zehr, J. P., Leung, S., Deng, L., and Liu, H.: High biomass
737 turnover rates of endosymbiotic nitrogen-fixing cyanobacteria in the western Bering Sea, *Limnology and Oceanography Letters*, 7, 501–
738 509, 2022.

739 Coale, T. H., Loconte, V., Turk-Kubo, K. A., Vanslembrouck, B., Mak, W. K. E., Cheung, S., Ekman, A., Chen, J.-H., Hagino, K., Takano,
740 Y., et al.: Nitrogen-fixing organelle in a marine alga, *Science*, 384, 217–222, 2024.

741 Dähnke, K. and Thamdrup, B.: Nitrogen isotope dynamics and fractionation during sedimentary denitrification in Boknis Eck, Baltic Sea,
742 *Biogeosciences*, 10, 3079–3088, 2013.

743 Damm, E., Helmke, E., Thoms, S., Schauer, U., Nöthig, E., Bakker, K., and Kiene, R.: Methane production in aerobic oligotrophic surface
744 water in the central Arctic Ocean, *Biogeosciences*, 7, 1099–1108, 2010.

745 Díez, B., Bergman, B., Pedrós-Alió, C., Antó, M., and Snoeijs, P.: High cyanobacterial *nifH* gene diversity in Arctic seawater and sea ice
746 brine, *Environmental microbiology reports*, 4, 360–366, 2012.

747 Emeis, K.-C., Mara, P., Schlarbaum, T., Möbius, J., Dähnke, K., Struck, U., Mihalopoulos, N., and Krom, M.: External N inputs and internal
748 N cycling traced by isotope ratios of nitrate, dissolved reduced nitrogen, and particulate nitrogen in the eastern Mediterranean Sea, *Journal*

749 of Geophysical Research: Biogeosciences, 115, 2010.

750 Falkowski, P. G., Fenchel, T., and Delong, E. F.: The microbial engines that drive Earth's biogeochemical cycles, science, 320, 1034–1039,
751 2008.

752 Farnelid, H., Andersson, A. F., Bertilsson, S., Al-Soud, W. A., Hansen, L. H., Sørensen, S., Steward, G. F., Hagström, Å., and Riemann, L.:
753 Nitrogenase gene amplicons from global marine surface waters are dominated by genes of non-cyanobacteria, PloS one, 6, e19 223, 2011.

754 Farnelid, H., Turk-Kubo, K., Ploug, H., Ossolinski, J. E., Collins, J. R., Van Mooy, B. A., and Zehr, J. P.: Diverse diazotrophs are present on
755 sinking particles in the North Pacific Subtropical Gyre, The ISME journal, 13, 170–182, 2019.

756 Fernández-Méndez, M., Turk-Kubo, K. A., Buttigieg, P. L., Rapp, J. Z., Krumpel, T., and Zehr, J. P.: Diazotroph diversity in the sea ice, melt
757 ponds, and surface waters of the Eurasian Basin of the Central Arctic Ocean, Frontiers in microbiology, 7, 217 140, 2016.

758 [Foster, R. A., Goebel, N. L., & Zehr, J. P.: Isolation of calothrix rhizosoleniae \(cyanobacteria\) strain SC01 from chaetoceros](#)
759 (bacillariophyta) spp. diatoms of the subtropical north pacific ocean 1. Journal of Phycology, 46(5), 1028-1037, 2010.

760 Foster, R. A., Kuypers, M. M., Vagner, T., Paerl, R. W., Musat, N., and Zehr, J. P.: Nitrogen fixation and transfer in open ocean diatom–
761 cyanobacterial symbioses, The ISME journal, 5, 1484–1493, 2011.

762 Foster, R. A., Tienken, D., Littmann, S., Whitehouse, M. J., Kuypers, M. M., and White, A. E.: The rate and fate of N2 and C fixation by
763 marine diatom-diazotroph symbioses, The ISME journal, 16, 477–487, 2022.

764 Fox, A. and Walker, B. D.: Sources and Cycling of Particulate Organic Matter in Baffin Bay: A Multi-Isotope $\delta^{13}\text{C}$, $\delta^{15}\text{N}$, and $\Delta^{14}\text{C}$
765 Approach, Frontiers in Marine Science, 9, 846 025, 2022.

766 Fu, L., Niu, B., Zhu, Z., Wu, S., and Cd-hit, W. L.: Accelerated for clustering the next-generation sequencing data, Bioinformatics, 28,
767 3150–3152, 2012.

768 Galloway, J., Dentener, F., Capone, D., Boyer, E., Howarth, R., Seitzinger, S., Asner, G., Cleveland, C., Green, P., Holland, E., et al.: Nitrogen
769 cycles: past, present, and future. Biogeochemistry 70, 153e226, 2004.

770 Garcia-Robledo, E., Corzo, A., and Papaspyrou, S.: A fast and direct spectrophotometric method for the sequential determination of nitrate
771 and nitrite at low concentrations in small volumes, Marine Chemistry, 162, 30–36, 2014.

772 [Geider, R. J., & La Roche, J.: Redfield revisited: variability of C \[ratio\] N \[ratio\] P in marine microalgae and its biochemical](#)
773 [basis. European Journal of Phycology, 37\(1\), 1-17, 2002.](#)

774 Gladish, C. V., Holland, D. M., and Lee, C. M.: Oceanic boundary conditions for Jakobshavn Glacier. Part II: Provenance and sources of
775 variability of Disko Bay and Ilulissat icefjord waters, 1990–2011, Journal of Physical Oceanography, 45, 33–63, 2015.

776 [Grosse, J., Bombar, D., Doan, H. N., Nguyen, L. N., & Voss, M.: The Mekong River plume fuels nitrogen fixation and determines](#)
777 [phytoplankton species distribution in the South China Sea during low and high discharge season. Limnology and Oceanography, 55\(4\),](#)
778 [1668-1680, 2010.](#)

779 Großkopf, T., Mohr, W., Baustian, T., Schunck, H., Gill, D., Kuypers, M. M., Lavik, G., Schmitz, R. A., Wallace, D. W., and LaRoche, J.:
780 Doubling of marine dinitrogen-fixation rates based on direct measurements, Nature, 488, 361–364, 2012.

781 Gruber, N.: The dynamics of the marine nitrogen cycle and its influence on atmospheric CO₂ variations, in: The ocean carbon cycle and
782 climate, pp. 97–148, Springer, 2004.

783 Gruber, N. and Galloway, J. N.: An Earth-system perspective of the global nitrogen cycle, Nature, 451, 293–296, 2008.

784 Gruber, N. and Sarmiento, J. L.: Global patterns of marine nitrogen fixation and denitrification, Global biogeochemical cycles, 11, 235–266,
785 1997.

Formatted: English (UK)

Formatted: Indent: Left: 0,14 cm, First line: 0 cm

Formatted: Font: Not Italic

Formatted: Font: Not Italic

Formatted

786 Haine, T. W., Curry, B., Gerdes, R., Hansen, E., Karcher, M., Lee, C., Rudels, B., Spreen, G., de Steur, L., Stewart, K. D., et al.: Arctic
787 freshwater export: Status, mechanisms, and prospects, *Global and Planetary Change*, 125, 13–35, 2015.

788 Hanna, E., Huybrechts, P., Steffen, K., Cappelen, J., Huff, R., Shuman, C., Irvine-Fynn, T., Wise, S., and Griffiths, M.: Increased runoff from
789 melt from the Greenland Ice Sheet: a response to global warming, *Journal of Climate*, 21, 331–341, 2008.

790 Hansen, M. O., Nielsen, T. G., Stedmon, C. A., and Munk, P.: Oceanographic regime shift during 1997 in Disko Bay, western Greenland,
791 *Limnology and Oceanography*, 57, 634–644, 2012.

792 Harding, K., Turk-Kubo, K. A., Sipler, R. E., Mills, M. M., Bronk, D. A., and Zehr, J. P.: Symbiotic unicellular cyanobacteria fix nitrogen in
793 the Arctic Ocean, *Proceedings of the National Academy of Sciences*, 115, 13 371–13 375, 2018.

794 Hawkings, J., Wadham, J., Tranter, M., Lawson, E., Sole, A., Cowton, T., Tedstone, A., Bartholomew, I., Nienow, P., Chandler, D., et al.:
795 The effect of warming climate on nutrient and solute export from the Greenland Ice Sheet, *Geochemical Perspectives Letters*, pp. 94–104,
796 2015.

797 Hawkings, J. R., Wadham, J. L., Tranter, M., Raiswell, R., Benning, L. G., Statham, P. J., Tedstone, A., Nienow, P., Lee, K., and Telling, J.:
798 Ice sheets as a significant source of highly reactive nanoparticulate iron to the oceans, *Nature communications*, 5, 1–8, 2014.

799 Hendry, K. R., Huvenne, V. A., Robinson, L. F., Annett, A., Badger, M., Jacobel, A. W., Ng, H. C., Opher, J., Pickering, R. A., Taylor, M. L.,
800 et al.: The biogeochemical impact of glacial meltwater from Southwest Greenland, *Progress in Oceanography*, 176, 102 126, 2019.

801 Holland, D. M., Thomas, R. H., De Young, B., Ribergaard, M. H., and Lyberth, B.: Acceleration of Jakobshavn Isbræ triggered by warm
802 subsurface ocean waters, *Nature geoscience*, 1, 659–664, 2008.

803 Hopwood, M. J., Connolly, D. P., Arendt, K. E., Juul-Pedersen, T., Stinchcombe, M. C., Meire, L., Esposito, M., and Krishna, R.: Seasonal
804 changes in Fe along a glaciated Greenlandic fjord, *Frontiers in Earth Science*, 4, 15, 2016.

805 Hyatt, D., Chen, G.-L., LoCascio, P. F., Land, M. L., Larimer, F. W., and Hauser, L. J.: Prodigal: prokaryotic gene recognition and translation
806 initiation site identification, *BMC bioinformatics*, 11, 1–11, 2010.

807 Jensen, H. M., Pedersen, L., Burmeister, A., and Winding Hansen, B.: Pelagic primary production during summer along 65 to 72 N off West
808 Greenland, *Polar Biology*, 21, 269–278, 1999.

809 Karl, D., Michaels, A., Bergman, B., Capone, D., Carpenter, E., Letelier, R., Lipschultz, F., Paerl, H., Sigman, D., and Stal, L.: Dinitrogen
810 fixation in the world's oceans, The nitrogen cycle at regional to global scales, pp. 47–98, 2002.

811 Knie, J.: Nitrogen isotope evidence for changing Arctic Ocean ventilation regimes during the Cenozoic, *Geophysical Research Letters*, 49,
812 e2022GL099 512, 2022.

813 Krawczyk, D. W., Yesson, C., Knutz, P., Arboe, N. H., Blicher, M. E., Zinglersen, K. B., and Wagnholt, J. N.: Seafloor habitats across
814 geological boundaries in Disko Bay, central West Greenland, *Estuarine, Coastal and Shelf Science*, 278, 108 087, 2022.

815 Krupke, A., Mohr, W., LaRoche, J., Fuchs, B. M., Amann, R. I., and Kuypers, M. M.: The effect of nutrients on carbon and nitrogen fixation
816 by the UCYN-A–haptophyte symbiosis, *The ISME journal*, 9, 1635–1647, 2015.

817 Laso Perez, R., Rivas Santisteban, J., Fernandez-Gonzalez, N., Mundy, C. J., Tamames, J., and Pedros-Alio, C.: Nitrogen cycling during an
818 Arctic bloom: from chemolithotrophy to nitrogen assimilation, *bioRxiv*, pp. 2024–02, 2024.

819 Lewis, K., Van Dijken, G., and Arrigo, K. R.: Changes in phytoplankton concentration now drive increased Arctic Ocean primary production,
820 *Science*, 369, 198–202, 2020.

821 Li, D., Liu, C.-M., Luo, R., Sadakane, K., and Lam, T.-W.: MEGAHIT: an ultra-fast single-node solution for large and complex metagenomics
822 assembly via succinct de Bruijn graph, *Bioinformatics*, 31, 1674–1676, 2015.

823 Löscher, C. R., Bourbonnais, A., Dekaezemacker, J., Charoenpong, C. N., Altabet, M. A., Bange, H. W., Czeschel, R., Hoffmann, C., and
824 Schmitz, R.: N₂ fixation in eddies of the eastern tropical South Pacific Ocean, *Biogeosciences*, 13, 2889–2899, 2016.

825 Löscher, C. R., Mohr, W., Bange, H. W., and Canfield, D. E.: No nitrogen fixation in the Bay of Bengal?, *Biogeosciences*, 17, 851–864, 2020.

826 Luo, Y.-W., Doney, S., Anderson, L., Benavides, M., Berman-Frank, I., Bode, A., Bonnet, S., Boström, K. H., Böttjer, D., Capone, D., et al.:
827 Database of diazotrophs in global ocean: abundance, biomass and nitrogen fixation rates, *Earth System Science Data*, 4, 47–73, 2012.

828 Martínez-Pérez, C., Mohr, W., Löscher, C. R., Dekaezemacker, J., Littmann, S., Yilmaz, P., Lehnen, N., Fuchs, B. M., Lavik, G., Schmitz,
829 R. A., et al.: The small unicellular diazotrophic symbiont, UCYN-A, is a key player in the marine nitrogen cycle, *Nature Microbiology*, 1,
830 1–7, 2016.

831 Mills, M. M., Turk-Kubo, K. A., van Dijken, G. L., Henke, B. A., Harding, K., Wilson, S. T., Arrigo, K. R., and Zehr, J. P.: Unusual marine
832 cyanobacteria/haptophyte symbiosis relies on N₂ fixation even in N-rich environments, *The ISME Journal*, 14, 2395–2406, 2020.

833 Mohr, W., Grosskopf, T., Wallace, D. W., and LaRoche, J.: Methodological underestimation of oceanic nitrogen fixation rates, *PLoS one*, 5,
834 e12 583, 2010.

835 Montoya, J. P.: Nitrogen stable isotopes in marine environments, *Nitrogen in the marine environment*, 2, 1277–1302, 2008.

836 Montoya, J. P., Carpenter, E. J., and Capone, D. G.: Nitrogen fixation and nitrogen isotope abundances in zooplankton of the oligotrophic
837 North Atlantic, *Limnology and Oceanography*, 47, 1617–1628, 2002.

838 Mortensen, J., Rysgaard, S., Winding, M., Juul-Pedersen, T., Arendt, K., Lund, H., Stuart-Lee, A., and Meire, L.: Multidecadal water mass
839 dynamics on the West Greenland Shelf, *Journal of Geophysical Research: Oceans*, 127, e2022JC018 724, 2022.

840 Munk, P., Nielsen, T. G., and Hansen, B. W.: Horizontal and vertical dynamics of zooplankton and larval fish communities during mid-
841 summer in Disko Bay, West Greenland, *Journal of Plankton Research*, 37, 554–570, 2015.

842 Murphy, J. and Riley, J. P.: A modified single solution method for the determination of phosphate in natural waters, *Analytica chimica acta*,
843 27, 31–36, 1962.

844 Myers, P. G. and Ribergaard, M. H.: Warming of the polar water layer in Disko Bay and potential impact on Jakobshavn Isbrae, *Journal of
845 Physical Oceanography*, 43, 2629–2640, 2013.

846 Patro, R., Duggal, G., Love, M. I., Irizarry, R. A., and Kingsford, C.: Salmon provides fast and bias-aware quantification of transcript
847 expression, *Nature methods*, 14, 417–419, 2017.

848 Redfield, A. C.: *On the proportions of organic derivatives in sea water and their relation to the composition of plankton (Vol. 1)*. Liverpool:
849 university press of liverpool, 1934.

850 Reeder, C. F., Stoltenberg, I., Javidpour, J., and Löscher, C. R.: Salinity as a key control on the diazotrophic community composition in the
851 Baltic Sea, *Ocean Science Discussions*, 2021, 1–30, 2021.

852 Rees, A. P., Gilbert, J. A., and Kelly-Gerrey, B. A.: Nitrogen fixation in the western English Channel (NE Atlantic ocean), *Marine Ecology
853 Progress Series*, 374, 7–12, 2009.

854 Rysgaard, S., Boone, W., Carlson, D., Sejr, M., Bendtsen, J., Juul-Pedersen, T., Lund, H., Meire, L., and Mortensen, J.: An updated view on
855 water masses on the pan-west Greenland continental shelf and their link to proglacial fjords, *Journal of Geophysical Research: Oceans*,
856 125, e2019JC015 564, 2020.

857 Schiøtt, S.: The Marine Ecosystem of Ilulissat Icefjord, Greenland, Ph.D. thesis, Department of Biology, Aarhus University, Denmark, 2023.

858 Schlitzer, R.: Ocean data view, 2022.

859 Schvarcz, C. R., Wilson, S. T., Caffin, M., Stancheva, R., Li, Q., Turk-Kubo, K. A., White, A. E., Karl, D. M., Zehr, J. P., and Steward, G. F.:

Formatted: Font: Not Italic

Formatted: Indent: Left: 0 cm, First line: 0 cm

Formatted

860 Overlooked and widespread pennate diatom-diazotroph symbioses in the sea, *Nature communications*, 13, 799, 2022.

861 Shao, Z., Xu, Y., Wang, H., Luo, W., Wang, L., Huang, Y., Agawin, N. S. R., Ahmed, A., Benavides, M., Bentzon-Tilia, M., et al.: Global
862 oceanic diazotroph database version 2 and elevated estimate of global N 2 fixation, *Earth System Science Data*, 15, 2023.

863 Sherwood, O. A., Davin, S. H., Lehmann, N., Buchwald, C., Edinger, E. N., Lehmann, M. F., and Kienast, M.: Stable isotope ratios in
864 seawater nitrate reflect the influence of Pacific water along the northwest Atlantic margin, *Biogeosciences*, 18, 4491–4510, 2021.

865 Shiozaki, T., Bombar, D., Riemann, L., Hashihama, F., Takeda, S., Yamaguchi, T., Ehama, M., Hamasaki, K., and Furuya, K.: Basin scale
866 variability of active diazotrophs and nitrogen fixation in the North Pacific, from the tropics to the subarctic Bering Sea, *Global Biogeochemical Cycles*, 31, 996–1009, 2017.

867 Shiozaki, T., Fujiwara, A., Ijichi, M., Harada, N., Nishino, S., Nishi, S., Nagata, T., and Hamasaki, K.: Diazotroph community structure and
868 the role of nitrogen fixation in the nitrogen cycle in the Chukchi Sea (western Arctic Ocean), *Limnology and Oceanography*, 63, 2191–
869 2205, 2018.

870 Shiozaki, T., Fujiwara, A., Inomura, K., Hirose, Y., Hashihama, F., and Harada, N.: Biological nitrogen fixation detected under Antarctic sea
871 ice, *Nature geoscience*, 13, 729–732, 2020.

872 Shiozaki, T., Nishimura, Y., Yoshizawa, S., Takami, H., Hamasaki, K., Fujiwara, A., Nishino, S., and Harada, N.: Distribution and survival
873 strategies of endemic and cosmopolitan diazotrophs in the Arctic Ocean, *The ISME journal*, 17, 1340–1350, 2023.

874 Sigman, D. M., DiFiore, P. J., Hain, M. P., Deutsch, C., Wang, Y., Karl, D. M., Knapp, A. N., Lehmann, M. F., and Pantoja, S.: The dual
875 isotopes of deep nitrate as a constraint on the cycle and budget of oceanic fixed nitrogen, *Deep Sea Research Part I: Oceanographic
876 Research Papers*, 56, 1419–1439, 2009.

877 Sipler, R. E., Gong, D., Baer, S. E., Sanderson, M. P., Roberts, Q. N., Mulholland, M. R., and Bronk, D. A.: Preliminary estimates of the
878 contribution of Arctic nitrogen fixation to the global nitrogen budget, *Limnology and Oceanography Letters*, 2, 159–166, 2017.

879 Slawyk, G., Collos, Y., and Auclair, J.-C.: The use of the 13C and 15N isotopes for the simultaneous measurement of carbon and nitrogen
880 turnover rates in marine phytoplankton 1, *Limnology and Oceanography*, 22, 925–932, 1977.

881 Sohm, J. A., Webb, E. A., and Capone, D. G.: Emerging patterns of marine nitrogen fixation, *Nature Reviews Microbiology*, 9, 499–508,
882 2011.

883 [Sterner, R. W., & Elser, J. J. Ecological stoichiometry: the biology of elements from molecules to the biosphere. In Ecological stoichiometry.](#)
884 [Princeton university press, 2017.](#)

885 Tang, W., Wang, S., Fonseca-Batista, D., Dehairs, F., Gifford, S., Gonzalez, A. G., Gallinari, M., Planquette, H., Sarthou, G., and Cassar, N.:
886 Revisiting the distribution of oceanic N2 fixation and estimating diazotrophic contribution to marine production, *Nature communications*,
887 10, 831, 2019.

888 Tremblay, J.-É. and Gagnon, J.: The effects of irradiance and nutrient supply on the productivity of Arctic waters: a perspective on climate
889 change, in: *Influence of climate change on the changing arctic and sub-arctic conditions*, pp. 73–93, Springer, 2009.

890 Turk, K. A., Rees, A. P., Zehr, J. P., Pereira, N., Swift, P., Shelley, R., Lohan, M., Woodward, E. M. S., and Gilbert, J.: Nitrogen fixation and
891 nitrogenase (nifH) expression in tropical waters of the eastern North Atlantic, *The ISME journal*, 5, 1201–1212, 2011.

892 Turk-Kubo, K. A., Frank, I. E., Hogan, M. E., Desnues, A., Bonnet, S., and Zehr, J. P.: Diazotroph community succession during the VAHINE
893 mesocosm experiment (New Caledonia lagoon), *Biogeosciences*, 12, 7435–7452, 2015.

894 Von Friesen, L. W. and Riemann, L.: Nitrogen fixation in a changing Arctic Ocean: an overlooked source of nitrogen?, *Frontiers in Microbi-
895 ology*, 11, 596 426, 2020.

Formatted: Font: Not Italic

Formatted: Condensed by 0.1 pt

897 Wang, S., Bailey, D., Lindsay, K., Moore, J., and Holland, M.: Impact of sea ice on the marine iron cycle and phytoplankton productivity,
898 Biogeosciences, 11, 4713–4731, 2014.

899 Zehr, J. P. and Capone, D. G.: Changing perspectives in marine nitrogen fixation, Science, 368, eaay9514, 2020.

Formatted: Condensed by 0.1 pt

